Chinese Journal of Chemical Engineering 88 (2025) 379–397

Contents lists available at ScienceDirect

Chinese Journal of Chemical Engineering

journal homepage: www.elsevier.com/locate/CJChE

Full Length Article

Novel polytriazole polymer membranes materials developed for the purification and separation of natural gas under high upstream feed pressure

Husnul Maab [1,*], Azra Touheed [2], Salman Salman [3], Maaz Khan [4]

[1] National Engineering and Scientific Commission (NESCOM), 2216 Islamabad, Pakistan
[2] Women University SWABI, 23561 KPK, Pakistan
[3] Baluchistan University of Engineering and Technology Khuzdar, 89100 Baluchistan, Pakistan
[4] Physics Division, PINSTECH, Nilore, 45650 Islamabad, Pakistan

ARTICLE INFO

Article history:
Received 23 March 2025
Received in revised form
16 June 2025
Accepted 17 June 2025
Available online 7 August 2025

Keywords:
Polymers
Membranes
Separation and purification
Natural gas
Water

ABSTRACT

The gas transport properties of both single and mixed gas systems including CH_4, CO_2, N_2, C_2H_6, and helium (He) were investigated using novel polymer membranes fabricated *via* solution casting from organic solvents. The fluorinated polytriazole polymers were synthesized through a polycondensation method incorporating hexafluoroisopropylidene the main polymer backbone, with various fluorinated aniline derivatives as side chains. It was observed that the bulky fluorinated aniline derivative groups such as 4-fluoroaniline, 2,5-difluoroaniline, 4-bromo-2,5-difluoroaniline, and 2,3,4,5,6-pentafluoroaniline significantly influenced the gas separation performance of the polymer membranes, particularly in terms of permeability and selectivity. The membranes exhibited excellent mechanical stability across a wide range of pure CO_2 feed pressures (100–800 psi, 1 psi = 6.895 kPa) without signs of plasticization, highlighting their robustness for high-pressure applications. Additionally, the polymer synthesis process is reproducible and can be readily scaled, with each material displaying high solubility in organic solvents such as dimethyl acetamide, chloroform, and *N*-methyl pyrrolidone. Compared to gases such as CH_4, N_2, and C_2H_6, the newly developed polymer membranes demonstrated superior permeability for CO_2 and He under upstream feed pressures of up to 800 psi. These materials represent a completely novel class of polymer membranes tailored for advanced gas purification technologies. Their enhanced separation performance, particularly for CO_2 removal and He recovery from natural gas streams at high processing pressures, positions them as promising candidates for industrial applications in gas purification and separation.

1. Introduction

The application of synthetic polymer membranes in natural gas purification and separation systems is currently the subject of extensive research. Numerous polymer membrane types have drawn a lot of interest and have a long history of use in industry as unique polymer membrane materials for the separation of constituents of natural gas. Unfortunately, under the operational experimental settings (pressure and gas systems), the majority of polymer membranes show poor mechanical, thermal, and chemical resistance, necessitating costly and time-consuming extra treatments like blending or chemical modification. High mechanical, thermal, and chemical stabilities of membrane materials allow them to withstand high upstream feed pressures, extend membrane life, and maintain membrane integrity under specific experimental settings related to gas separation and purification technologies. Thus, it is especially desirable to develop novel polymer materials for membrane-based gas separation methods.

Nitrogen (N_2), water (H_2O), heavy hydrocarbons (C_{3+}), carbon dioxide (CO_2), hydrogen sulfide (H_2S), and other contaminants can be found in natural gas in amounts ranging from less than 1% to more than 50%. Therefore, in order to meet pipeline and burner

* Corresponding author.
E-mail address: maabkhan@gmail.com (H. Maab).

https://doi.org/10.1016/j.cjche.2025.06.022

quality criteria and to fully utilize natural gas, the methane gas (CH_4) needs to be cleaned by removing such contaminants. In comparison to current conventional gas purification technologies like pressure swing absorption (PSA) and amine treatment process, the natural gas sweetening process, which includes acid gas removal with the membranes-based or a membrane-absorption hybrid process, has emerged as one of the efficient separation technologies due to its environment friendliness, low capital and operation cost, high energy saving, small and compact size, and economic feasibility [1–10]. Nevertheless, there are still certain insufficient performance issues with polymer membranes that prevent their use and manufacture on a commercial scale [5–13].

Obtaining high permeability and high selectivity for the CO_2/CH_4 target gas pair is one of these obstacles. Other ones include physical aging and membrane material plasticization with rising upstream input pressure, as well as comparison with the trade-off curve. Currently, the primary challenge in the advancement of polymer membrane materials, particularly in the removal of acid gases (H_2S and CO_2), is the plasticization of membranes when subjected to the specified upstream gas feed pressure. The condition known as "plasticization" occurs when an acid gas (often CO_2) is fed into a polymer membrane at a high upstream pressure, causing the membrane to stretch and lose its permselectivity for a particular gas pair [4,13–18]. The development of polymer membrane materials with great mechanical and chemical stability has attracted a lot of attention. Many resources have been used in this area to create polymer membrane materials that are highly stable both mechanically and chemically so they can withstand upstream feed pressure without sacrificing gas permeability or selectivity [17,18]. Some of the most widely used polymer materials created for natural gas processing are glassy and rubbery membranes, including poly-dimethyl siloxane, cellulose acetate, cellulose esters, nitrocellulose, polymers with intrinsic microporosity, polysulfones, polycarbonate, Pebax, polyether sulfone, polyamide, polyacrylonitrile, polyamide, and others. These materials were studied for different mixes of natural gas and syngas separation and purification processes under different experimental settings [1–33].

The fabrication of a promising material with high performance efficiency in terms of permeability and selectivity for a target gas pair is often the goal of any new materials for membrane applications or chemical modifications to existing membrane materials. An increase in gas permeability always compromises with a significant decrease in gas pair selectivity, despite the significant efforts made to develop a membrane material with the desired properties and high-performance efficiency (perm-selectivity for a target gas pair). These challenges make it difficult to develop and fabricate polymer membrane materials that simultaneously exhibit high gas permeabilities and selectivities. This inherent trade-off significantly limits the practical efficiency of such membranes. Moreover, these limitations hinder the industrial deployment and large-scale manufacturing of polymer membranes, especially for high-pressure field applications where mechanical and separation performance must be rigorously maintained.

Polytriazole polymers are those that contain a triazole ring either as a side chain or in their backbone. The structure of the triazole ring is akin to a furan, with two carbon atoms and three nitrogen atoms joined by double bonds. Since the triazole ring is hydrogen atom free, it functions as an electron-withdrawing group in polymers. These rings give polymers unique qualities like low dielectric constant, high glass transition temperature, good hydrolytic stability, high thermal, mechanical, and chemical stability, and lack of rearrangement and flexibility. Because of these qualities, polytriazole polymers are regarded as high-performance materials. They have been studied for difficult applications such as fire retardants, flame-retardants, and potentially useful membrane materials for water purification [19–27]. The literature contains some early research on the synthesis of polytriazole, which was followed by studies on single gas permeation [26,27,29]. On the other hand, no substantial research has been done on various polytriazole polymer membrane chemistries for mixed gas systems at noticeably high feed pressures. Chisca *et al.* [31] have published a study on the heat treatment of polytriazole membranes functionalized with hydroxyl (OH). The work concentrated on thermally cross-linking OH-functionalized polytriazole films and then converting them *via* a series of stages into carbon molecular sieves. They contrasted the pristine polytriazole polymer membranes with thermally treated films to see how well they separated gases. A range of high upstream feed pressures, from 100 to 800 psi (1 psi = 6.895 kPa), were tested for single and mixed gas systems (CO_2, CH_4, N_2, and C_2H_6) [30].

We have developed a series of novel polytriazole membrane materials incorporating hexafluoroisopropylidene (HFA) and a triazole ring, along with various bulky fluorinated aniline derivative groups integrated into the polymer backbone. These findings are presented in our recent publications [30–42].

To systematically optimize membrane properties, different aniline derivatives with an increasing number of fluorine atoms in the fluorinated polytriazole polymers (FPTA-1 to FPTA-4) were incorporated into the polymer as side-chain functional groups. The highly electronegative fluorine atoms introduced electrostatic repulsion between polymer segments, effectively increasing the fractional free volume (FFV) within the membrane matrix. This structural modification significantly enhanced CO_2 permeability, allowing for efficient gas transport while maintaining high selectivity and a key breakthrough in overcoming traditional permeability–selectivity trade-offs. The designed membrane materials exhibit low penetration for CH_4, C_2H_6, and N_2, while demonstrating exceptional permeability for helium (He) and CO_2. Additionally, these materials display remarkable resistance to plasticization, as validated through long-term testing under pure CO_2 upstream pressures up to 800 psi, with no swelling, dilatation, or mechanical deterioration observed.

Encouraged by these findings, we expanded our investigation into customized fluorinated polytriazole chemistries for advanced natural gas separation technologies, aiming for high permeability and gas-pair selectivity.

Fig. 1 illustrates the chemical composition of fluorinated polytriazole (FPTA) polymers, highlighting their triazole ring, HFA backbone, and bulky fluorinated aniline side chains, which contribute to exceptional gas separation performance.

2. Experimental

2.1. Chemical components

4,4-(Hexafluoroisopropylidene, HFA, 99%, Aldrich), hydrazine sulphate (HS, 98%, Aldrich), 4-fluoroaniline (99%, Aldrich), 2,5-difluoroaniline (99%, Aldrich), 4-bromo-2,5-difluoroaniline (99%, Aldrich), 2,3,4,5,6-pentafluoroaniline (99%, Aldrich), *N*-methyl pyrolidone (NMP, 99%, Aldrich), chloroform (99%, Aldrich), polyphosphoric acid (PPA, ca 84% as P_2O_5, from Alfa Aesar) and sodium hydroxide (NaOH, 99%, Aldrich) were used for polymers synthesis and membrane fabrication as received.

2.2. FPTA polymer synthesis

As per the synthesis technique previously indicated in our earlier work [4,13–17,23–30], FPTA polymers containing various

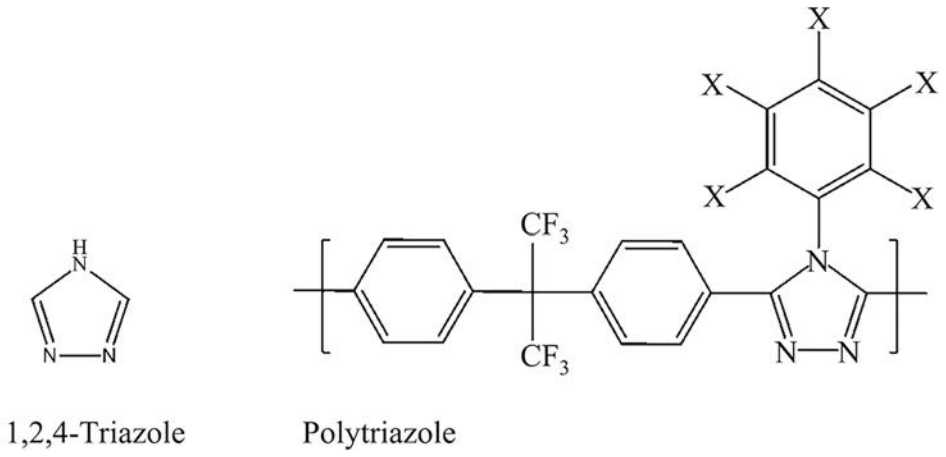

Fig. 1. Chemical structures of a triazole ring and polytriazole polymer (X = H, F, C, Br *etc.*).

groups of fluorinated aniline derivatives were synthesized in the lab. A two-step polymer synthesis process was used to develop all of the polymers. The first phase involved the production of fluorinated polyoxadiazole (FPOD), and the second step involved the synthesis of FPTA polymers.

2.2.1. FPOD polymer synthesis

PPA was used as a solvent in a 100 ml three-necked round-bottom flask. It was then heated to 100 °C for an hour while being vigorously stirred by hand and continuously purged with dry, pure N_2 gas to eliminate any remaining water from the reaction system. Following the addition of the first monomer, HS, to the solvent system, the temperature was increased to 160 °C while vigorous stirring was done to fully mix and dissolve the HS in the PPA solvent. The second monomer, HFA, was added to the reaction solution right away at 160 °C. For almost 3 h, there was a steady flow of pure, dry N_2 gas while vigorous mechanical stirring was performed. The molar monomer ratio of HS/HFA and the molar ratio of PPA/HS were maintained at 1.2 and 30, respectively. A colorless (white) viscous polymer was the end result, which was precipitated by adding it to a basic solution of 1 $mol \cdot L^{-1}$ NaOH and stirring constantly for an hour to eliminate any remaining acid. After filtering, the fibrous polymer that was produced was placed in distilled water and allowed overnight at 80 °C to completely eliminate any remaining base and bring the water's pH level down to neutral. Ultimately, the polymer was vacuum-dried for 24 h at 100 °C in an oven. FPTA were synthesized using this polymer, which is also known as HFA-based polyoxadiazole (FPOD). The structure and synthesis process of FPOD polymer's reaction can be viewed in Fig. 2.

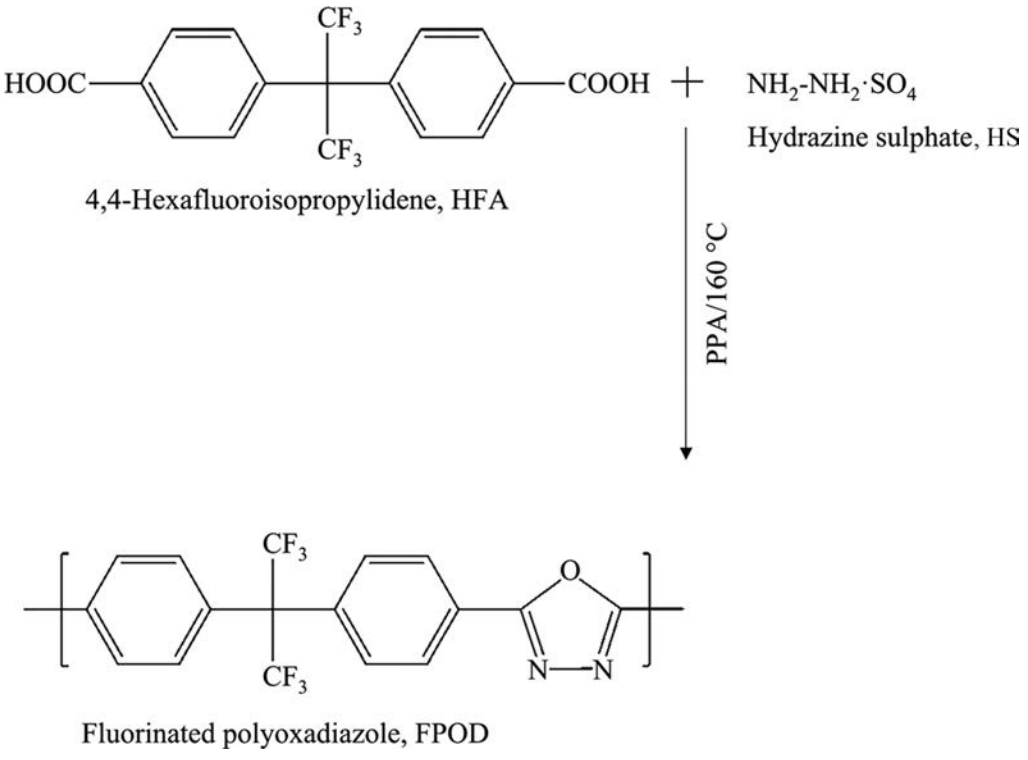

Fig. 2. Monomers and reaction scheme of FPOD synthesis.

2.2.2. Synthesis of FPTA polymers

The reaction solvent, NMP, was introduced to a 250 ml flask with three necks and a round bottom. The flask was heated to 100 °C for an hour while being vigorously stirred mechanically. To eliminate any water content, the reaction system was purged with clean, dry N_2 gas. Following the addition of the FPOD polymer, the solvent system was heated to 190 °C, allowing for vigorous stirring to thoroughly mix and dissolve the polymer in NMP solvent. The reaction system was immediately brought to 190 °C, and 1.0 g of PPA was added as a catalyst along with the monomer, 4-fluoroaniline. The reaction was vigorously stirred for 3 to 5 h while pure and dry N_2 gas was continuously supplied. The molar monomer ratio of FPOD/monomer and the ratio of NMP/FPOD were maintained at 1.2 and 20, respectively, in order to fully utilize the additional polymer. The end result was a viscous polymer with a dark blue color that was precipitated by putting it into 5.0 L of distilled water and rapidly stirring it for an hour to eliminate all of the solvent. The fibrous polymer was then filtered and placed in distilled water, where it was washed overnight at 80 °C to eliminate any remaining solvent residue. Ultimately, the polymer was vacuum-dried for 24 h at 190 °C in an oven.

Using selected fluorinated aniline derivatives namely 2,5-difluoroaniline, 4-bromo-2,5-difluoroaniline, and 2,3,4,5,6-pentafluoroaniline as monomers, additional structurally distinct FPTA polymers were synthesized *via* the same polymerization strategy. In total, five FPTA polymers were successfully synthesized and subsequently investigated for their gas separation performance as part of this study. Figs. 3–6 illustrate the overall synthetic route, the selected monomers, and the resulting chemical structures of the FPTA polymers, including their corresponding IUPAC names.

2.3. Manufacturing of dense membranes

Polymer membranes that were both dense and symmetric were produced using the solution casting process. The polymers were thoroughly dissolved in (2% (mass)) chloroform solvent and forcefully mixed and agitated for 24 h at room temperature in order to prepare a homogenous solution for the membrane construction process. Since the parameters of the solution casting and polymer solution preparation directly impact the intrinsic properties of the membranes, great care was taken in their manufacture. Filtration of the polymer solutions was done using a 0.45 μm thick filter. A sanitized glass Petri dish of a predetermined size was filled with a polymer solution to produce dense and symmetric membranes. For the purpose of later drying the solvent *via* evaporation at room temperature, all the plates were put inside an oven. Dishes were put inside an oven to evaporate the solvent at room temperature while nitrogen gas was purged of an inert and dry environment for a full day. To eliminate any remaining solvent, membranes were further dried by applying suction for an entire night in a vacuum oven set at a higher temperature of 150 °C. Inside the oven, the membranes were cooled to ambient

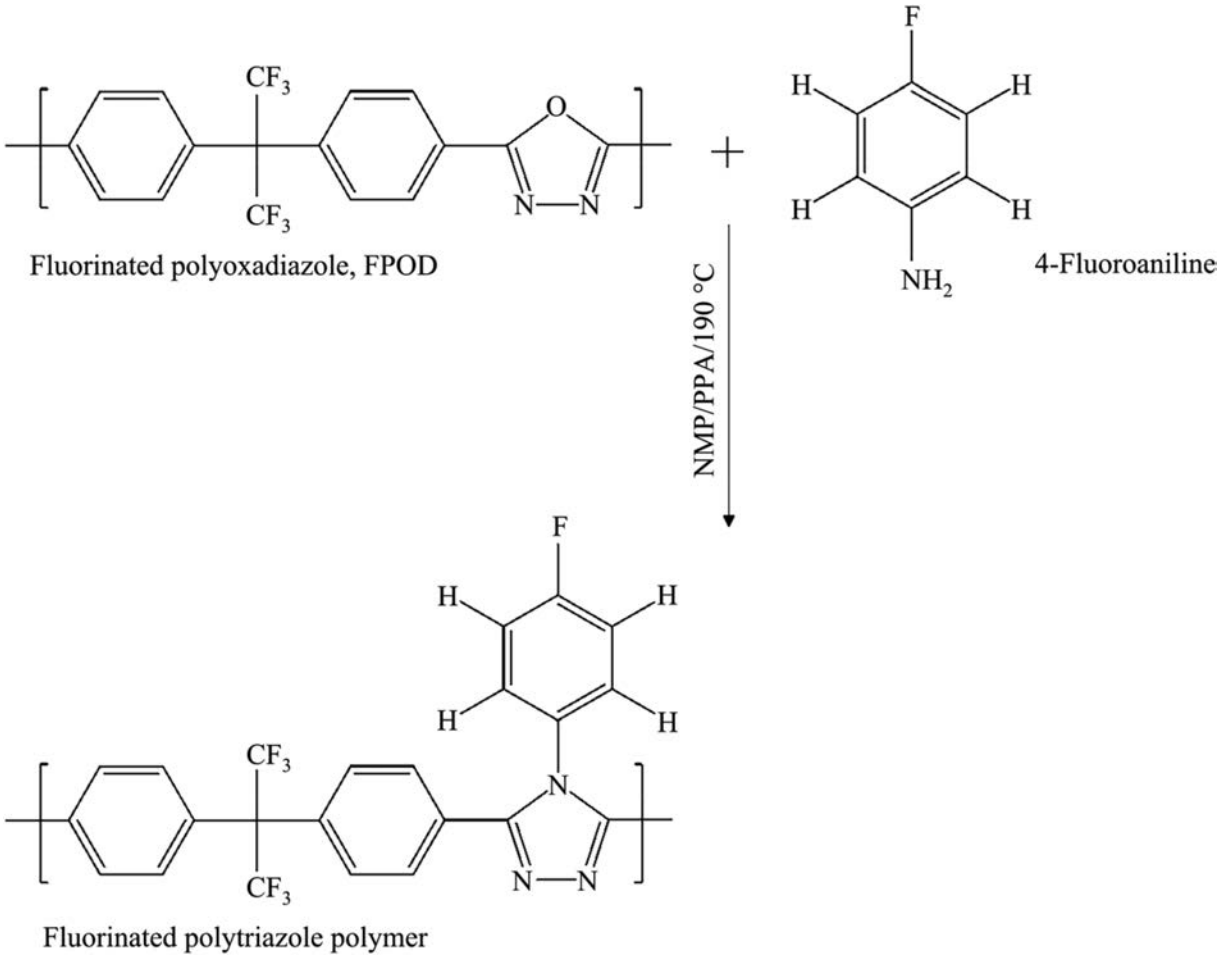

Fig. 3. Synthesis scheme of polytriazole polymers.

temperature in an inert N_2 gas atmosphere. The thickness of the membrane was between 50 and 60 μm.

2.4. Characterizations

Nuclear magnetic resonance (NMR) spectroscopy was used to assess and validate the polymer production. Using a homogenous solution of polymers in chloroform-d and tetramethyl silane (TMS) as an internal standard (0), C NMR spectra were obtained at 25 °C using a Bruker Advance III-700MHz (Germany) liquid NMR apparatus equipped with a TCI cryprobe (Z-axis gradient) model.

^{13}C NMR (FPOD in chloroform-d): δ164.1 (C1).

^{13}C NMR (FPTA-1 in chloroform-d): δ163.2 (C1), 116.3 (C2), 153.3 (C3).

^{13}C NMR (FPTA-2 in chloroform-d): δ158.5 (C1), 161.3 (C2), 153.3 (C3).

^{13}C NMR (FPTA-3 in chloroform-d): δ112.7 (C1), 161.7 (C2), 153.3 (C3), 163.5 (C4).

^{13}C NMR (FPTA-4 in chloroform-d): δ143.3 (C1), 137.3 (C2), 153.3 (C3).

Gel permeation chromatography (GPC) using an Agilent 1200 (USA) series instrument with UV and RI detectors and a column fitted with PLgel olexis (7.5 mm_300 mm) was used to determine the average molecular weight of the produced polymers. The polystyrene standards that Merck provided were used to calibrate the equipment. A 1000 mg·L^{-1} polymer solution was injected at a 1 ml·min^{-1} flow rate.

To verify the thermal stability of polymers and any solvent residue remaining inside the membrane's matrix, thermogravimetric analysis (TGA) was performed using a STA 449 F3 instrument (Netzsch, Germany). Every sample of fluorinated polymers and membranes was heated at a rate of 10 °C·min^{-1} from 30 to 650 °C, followed by an inert and dry N_2 gas purge. The glass transition temperature (T_g) of the fluorinated polymer membrane samples was also ascertained using dynamic mechanical thermal analysis (DMTA) on an RSA-III TA-instrument (USA) operating in the film tension mode at a frequency of 1 Hz. Every membrane sample was subjected to analysis at a constant strain of 0.05% and a temperature increase of 5 °C·min^{-1} between 30 and 350 °C.

A Mettler Toledo (Switzerland) density meter was used to measure the fluorinated polymer membranes' density at room temperature. For results that could be replicated, each measurement was done at least three times. Membrane strips of known mass that were small and dried floated in a liquid called cyclohexane. Using Bondi's group contribution method, the membrane samples' fractional free volumes (FFV) were computed [32,34,35]. The given Eq. (1) was used to compute the fluorinated polymer membranes' FFV.

$$FFV = (V - 1.3V_w) / V \quad (1)$$

where, V (cm^3·g^{-1}) is the specific volume of a polymer and is equal to $1/\rho$, and ρ (g·cm^{-3}) is the polymer density. V_w is the van der Waals volume determined by the sum of atomic and bond contributions method [34,35]. In general, this FFV explain the transport correlation inside a polymer matrix as illustrated in Fig. 7.

2.5. Characterization of the membranes' gas permeability

Our earlier papers [29–32] provide a thorough explanation of the single and mixed gas permeation studies of the polymer membranes along with the setup and permeation cell design in detail. Fig. 8 illustrates the constant pressure (CP)/variable volume apparatus used for all of the gas permeation tests for the FPTA polymer membranes. The single and mixed gas characterization studies were conducted at ambient temperature with upstream

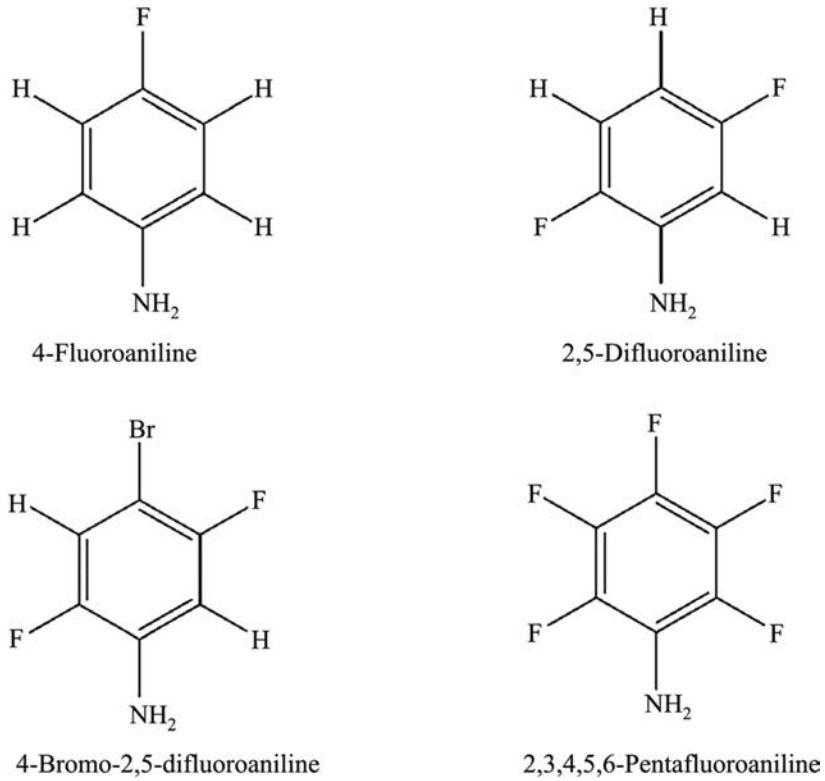

Fig. 4. Different fluorinated aniline derivatives.

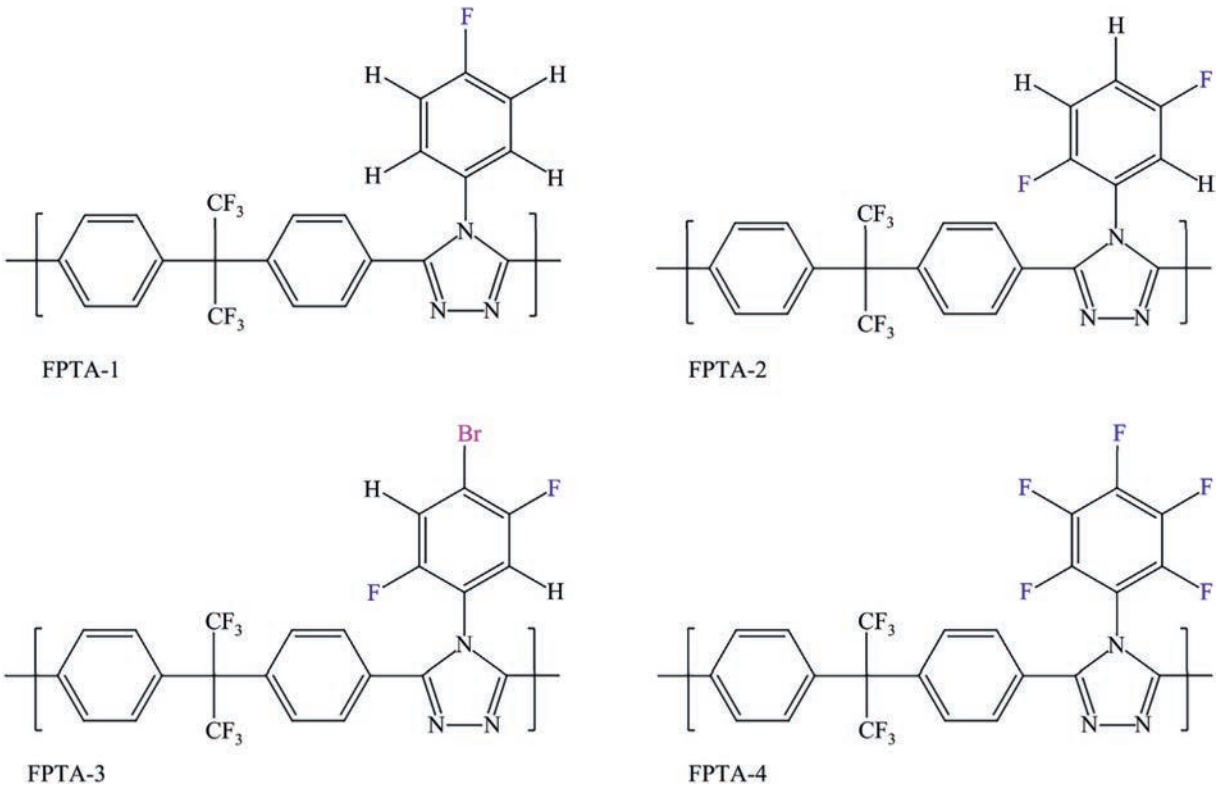

Fig. 5. Chemical structures of FPTA polymers.

FPTA-1	Poly(4-(4-fluorophenyl)-3-(4-(1,1,1,3,3,3-hexafluoro-2-(*p*-tolyl)propan-2-yl)phenyl)-5-methyl-4H-1,2,4-triazole)
FPTA-2	Poly(4-(2,5-difluorophenyl)-3-(4-(1,1,1,3,3,3-hexafluoro-2-phenylpropan-2-yl)phenyl)-4H-1,2,4-triazole)
FPTA-3	Poly (4-(4-bromo-2,5-difluorophenyl)-3-(4-(1,1,1,3,3,3-hexafluoro-2-(*p*-tolyl)propan-2-yl)phenyl)-5-methyl-4H-1,2,4-triazole)
FPTA-4	Poly (3-(4-(1,1,1,3,3,3-hexafluoro-2-(*p*-tolyl)propan-2-yl)phenyl)-5-methyl-4-(perfluorophenyl)-4H-1,2,4-triazole)

Fig. 6. IUPAC nomenclature of polymers.

feed side pressures ranging from 100 to 800 psi and a permeate side at normal atmospheric pressure.

Micro gas chromatography was used to analyze the composition of the retentate and permeate from the mixed gas system. An area of about 12 cm^2 of membrane film was mounted, sealed with epoxy glue, and masking with an aluminum tap inside a measurement cell to guarantee that the gas permeation will not bypass the membrane area. Three membrane samples from each polymer material were tested simultaneously at each operating condition to ensure that no defects in membranes were present. Prior to the original measurements, all of the membranes were conditioned with gases (single or mixed) for 48 h, after which each measurement was made after an extended period of 10 h, with a permeability coefficient inaccuracy of less than ±5% of the displayed values.

Solution-diffusion model of gas movement [1] *via* a densely symmetric membrane is a pressure-driven mechanism where the gas flux (J) is inversely proportional to the membrane's thickness (L) but proportionate to the pressure differential between the upstream feed pressure (p_1) and the downward permeate pressure (p_2). One inherent attribute of the material is the permeability (P) of a gas component through the dense symmetric membrane sheet. However, testing parameters including temperature, upstream feed pressure, and interactions between the polymer and gas molecules can alter the characteristics of the membrane material, changing its permeability.

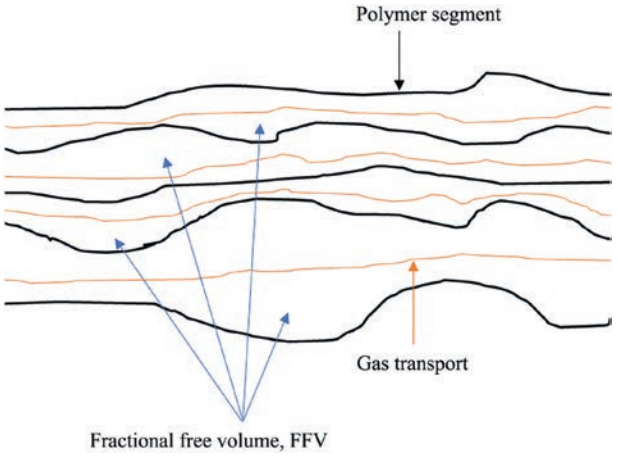

Fig. 7. The FFV within the polymer membrane.

$$J = P \times \frac{p_1 - p_2}{L} \tag{2}$$

The membranes permeability coefficient and selectivity of each gas component in the mixture at a set pressure condition were calculated from Eqs. (3) and (4) below.

$$P = D \times S = \frac{X_{perm} \times J_{perm} \times L}{\left(P_{feed} \times X_{feed} - P_{perm} \times X_{perm}\right)} \tag{3}$$

$$\text{Selectivity } (\alpha_{ab}) = \frac{P_a}{P_b} = \frac{S_a}{S_b} \times \frac{D_a}{D_b} \tag{4}$$

where X_{perm} and X_{feed} represents the mole fraction of gas components in the permeate and feed stream, respectively. J_{perm} ($cm^3 \cdot cm^{-2} \cdot s^{-1}$) represents the total permeate flux, P_{feed} and P_{perm} are the pressures (cmHg absolute, 1 cmHg = 1333.22 Pa) on the feed and permeate side of the membrane, respectively. L (cm) represents the membrane thickness while $\left(\frac{S_a}{S_b} \times \frac{D_a}{D_b}\right)$ are solubility and diffusivity selectivities of the two gases under test conditions. The diffusivity (D) of a gas mainly depends on the available free volume in between the polymer segments and the molecular size of a gas component, while the gas solubility depends mainly on the interaction of a gas component with the polymer materials. The membrane ability to separate two or more gaseous components is a very important parameter and is called as ideal selectivity or perm-selectivity and is expressed as Eq. (4). The P unit is known as Barrer and 1 Barrer = 10^{-10} $cm^3(STP) \cdot cm \cdot cm^{-2} \cdot s^{-1} \cdot cmHg^{-1}$.

3. Results and Discussion

3.1. ^{13}C NMR characterization of polymers

Fig. 9 displays the fluorinated polyoxadiazole ^{13}C NMR spectra. Strong chemical shift at 164.11 (C1) indicated that the polycondensation process between the monomers HFA and HS, produced the fluorinated polyoxadiazole polymer. The carbon atoms from the oxadiazole ring, which is contained in the polymer backbone, are responsible for this chemical shift (164) [26,27]. The ^{13}C NMR spectra for FPTA polymers produced in this work for gas characterizations are shown in Figs. 10–13. The fluorinated aniline derivative's effective substitution process (Fig. 4) on the fluorinated polyoxadiazole polymers was confirmed by the substantial chemical shifts at 153.3 (C3). For all of the FPTA polymers made in this work, a chemical shift at 153.3 was detected, which corresponds to the carbon atom of the triazole ring of the main stem of the polymer (Fig. 5). The carbon atoms of the side aromatic ring connected to the triazole ring of the polymers are represented by the chemical shifts at 163.2, 158.5, 161.3, 112.7, 161.7, 153.3, 163.5, 124.1, 130.0, 143.3, and 137.3. This further supports the successful substitution reaction between the fluorinated aniline derivatives and fluorinated polyoxadiazole polymer.

The thermal resistivity and stability of the polymers developed for this study were examined using thermogravimetric analysis (TGA) (Fig. 14). Table 1 displays the thermal dissociation temperatures (T_d) under the inert N_2 environment at 5% mass loss. The T_d values and TGA analysis curves demonstrate the strong thermal resistivity and stability of all the FPTA polymers in the 450–500 °C temperature range. The TGA curves demonstrate that mass loss as a result of degradation began around 450 °C and that there is a single degradation temperature for all polymer materials after 450 °C. Additionally, this verifies that there isn't any leftover solvent in the polymer membrane matrices that could compromise the membrane's functionality in gas characterization tests. The glass transition temperature (T_g) of polymers was also calculated using the DSC methodology, however no T_g was found for any of the polymers using this method. The high T_g values and the closeness to the polymer degradation temperature may be the cause. We have also seen similar behavior for several polyazole polymer materials in our earlier study [13,29,31,33].

The thermograms for the DMTA of all the materials containing FPTA polymers that were examined in order to ascertain the polymer glass transition temperature are displayed in Fig. 15. This

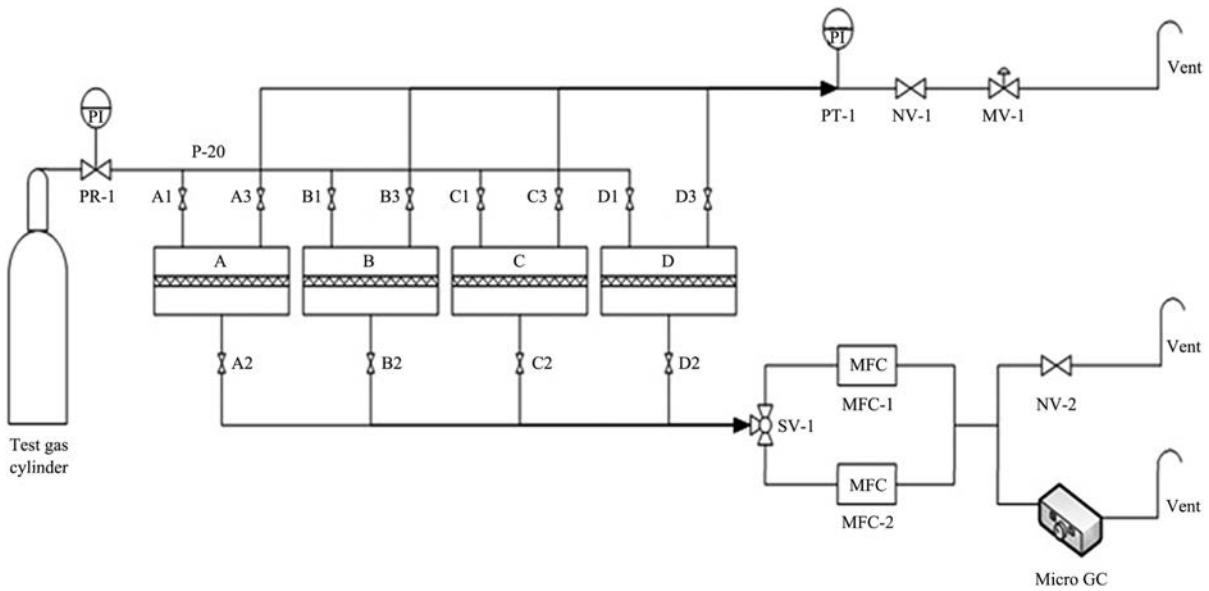

Fig. 8. A system with variable volume and constant pressure (CP) is used to measure the single and mixed gas penetration characteristics of membranes. PT-1 (pressure transducer); NV-1 and NV-2 (needle valves); A1, A3, B1, B3, C1, C3, D1 and D3 (gas inlet); A2, B2, C2 and D2 (permeate outlet); A, B, C, and D (membrane cells); MFC1 and MFC2 (mass flow controllers) [29–37].

approach detects the deformation of thin films caused by the applied stretching force by applying an extra tension force to the thin film through the probe. The materials used to make the polymer films had T_g that ranged from 200.5 to 225.3 °C. Fluorine atoms carrying bulky aniline derivatives and a triazole ring are the primary causes of these elevated T_g values. As was previously covered in depth, these groups (triazoles) provide these polymers some unique features.

Gel permeation chromatography (GPC) was used to determine the molecular weight of the polymers, which were found to be in the order of 103 $g \cdot mol^{-1}$. Table 2 displays PDI values that are a bit higher than 2. High molecular weight polymers in the 65–70 °C range comprise a side chain of fluorinated bulky aniline derivative groups and a backbone consisting of a triazole ring and HFA. Regardless of the molecular weights, all synthesized FPTA polymers produced dense membranes with strong mechanical and thermal stabilities.

3.2. Tests for single gas permeation

The permeation characteristics of single gases (CO_2, CH_4, N_2, and He) were investigated on all of the synthesized polymers (FPTA-1, FPTA-2, FPTA-3, and FPTA-4) membranes using a CP device. The findings were obtained at room temperature and under a constant upstream feed pressure of 100 psi. Table 3 displays the selectivities and permeation coefficient data for the tested single gases. The permeabilities of all the FPTA polymer membranes were significantly high for He and CO_2 gases, and extremely low for other individual gases including N_2 and CH_4. For the investigated FPTA polymer membrane materials, the selectivity coefficients of (CO_2/CH_4) and (He/CH_4) were notably high at this pressure (100 psi). Table 1 displays the FFV of every polymer that was produced for this study. As the amount of halogen atoms (fluorine atoms) on the side aniline derivatives group increases, the FFV rises (0.11 to 0.31). The bulky aniline derivative group as a side chain and the HFA moiety in the backbone of all synthesized FPTA polymers work together to reduce the ability of polymer segments to pack together, increasing the solubility of CO_2 and He relative to other single gases and improving the permeation and selectivity properties of polymer membranes. All of the synthesized FPTA polymeric membranes were further examined for comprehensive gas separation capabilities at a wide range of high upstream feed pressure (up to 800 psi) at room temperature due to the high permeability of CO_2 & He gases.

3.2.1. Single-gas permeation properties and the impact of upstream feed pressure

The permeation properties of single gases (CO_2, CH_4, N_2, and He) were assessed for all the produced polymer (FPTA) membrane materials at ambient temperature and within an upstream feed pressure range of 100 to 800 psi.

For FPTA-1, the permeability of N_2 and CH_4 gases did not significantly alter between 100 and 800 psi of applied pressure. For the two individual gases (CH_4 and N_2), the maximum permeability coefficients found were 4.72 and 4.30 Barrer at 800 psi. At 100 psi, the permeability coefficient for pure carbon dioxide gas (CO_2) was found to be 132.10 Barrer. As the upstream feed pressure increased from 100 to 800 psi, the permeability coefficient steadily decreased. The CO_2 gas's permeability coefficient was 125.11 Barrer at 800 psi. When pressure is increased from 100 to 800 psi, the selectivity of CO_2/CH_4 and He/CH_4 keeps declining. Table 4 displays the permeabilities and selectivities data for FPTA-1 polymer membranes.

For pure penetrant gases like CH_4 and N_2, the permeability coefficients (2.35 and 3.11 Barrer) for the dense membranes made from FPTA-2 polymer exhibited the same behavior over the applied upstream feed pressure range of 100 to 800 psi. The highest permeability coefficients measured at 100 psi for the pure single gases CO_2 and He were 185.23 and 285.55 Barrer, respectively. Because there was no apparent change in the permeability (2.35 Barrer) of pure methane at the applied feed pressure of 100 psi, the maximal ideal selectivities (He/CH_4) and (CO_2/CH_4) were measured up to 121.50 and 78.82, respectively. Meanwhile, when feed pressure increased from 100 to 800 psi, the selectivity coefficients of CO_2/CH_4 and He/CH_4 as well as the permeability coefficients for pure gas (CO_2 and He) declined. Compared to the earlier polymer (FPTA-1), the permeability and selectivity coefficient values for this polymer (FPTA-2) were significantly greater. The presence of an extra fluorine atom as a side chain on the bulky aniline derivative group increases more free volume (Table 1) inside the membrane matrix by lowering the likelihood of chain

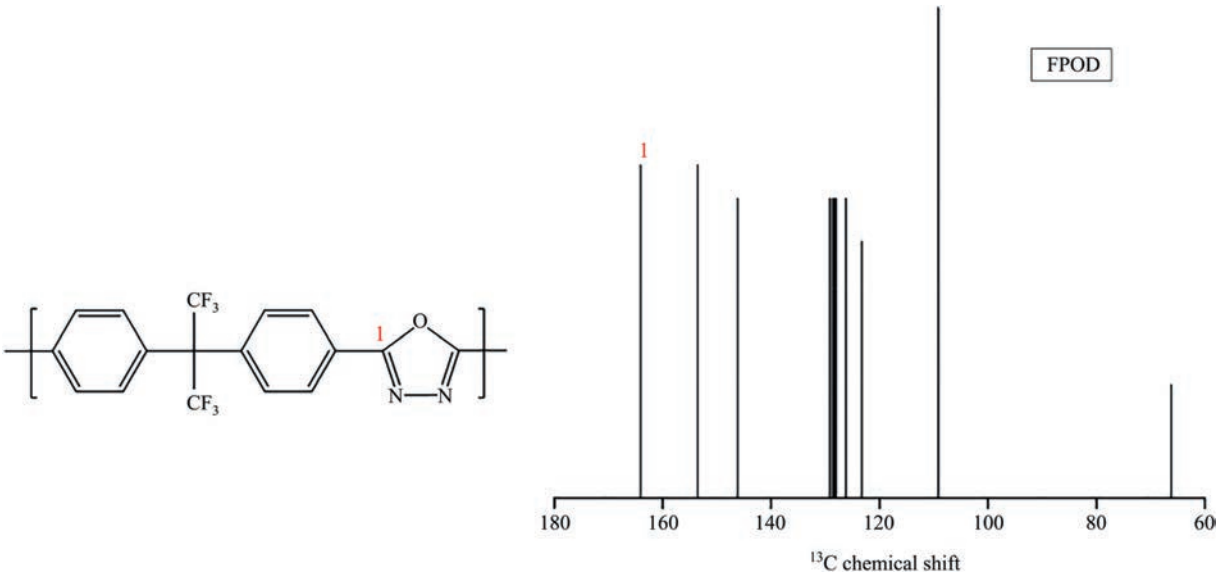

Fig. 9. ^{13}C NMR spectra of FPOD polymer.

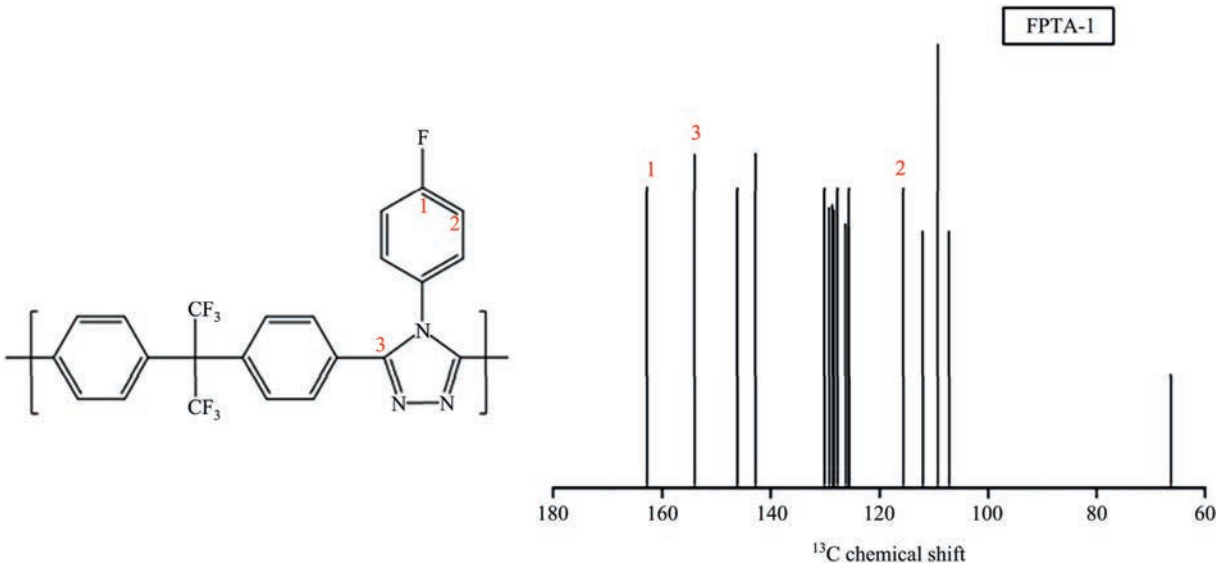

Fig. 10. Fluorinated polytriazole polymer's (FPTA-1) ^{13}C NMR spectra.

packing, which accounts for the superior performance of these polymer membranes. The statistics on selectivity and permeability are shown in Table 5.

A distinct behavior was seen for the membrane's polymer-prepared materials (FPTA-3), where a gradual increase in upstream feed pressure from 100 to 800 psi resulted in a slight decrease in the permeability coefficient of pure nitrogen gas and a slight increase in the permeability coefficient of pure CH_4. At 100 psi, the permeability values for individual gases, such as CO_2 and He, were found to be 240.24 and 305.21 Barrer, respectively. Between 100 and 800 psi of applied upstream feed pressure, a small drop in the permeability coefficient values of both CO_2 and He was noted. At the same upstream feed pressure of 100 psi, the optimum selectivities of (CO_2/CH_4) and (He/CH_4) were found to be 94.21 and 119.69, respectively. Under the applied upstream feed pressure range of 100 to 800 psi, the optimum selectivity of both (CO_2/CH_4) and (He/CH_4) decreased due to a slight rise in the permeability of CH_4 and a slight drop in the permeability values of bothCO_2 and He. In comparison to the earlier polymers (FPTA-1 and FPTA-2), the performance of this polymer (FPTA-3) membrane material towards acid gas (CO_2) removal was significantly superior in terms of permeability and selectivity. The aniline derivative group has two fluorine atoms (Br & F) and bromine as a bulky side chain moiety on the backbone. Since the two fluorine atoms (Br & F) on the aniline derivative group are highly electronegative, their presence as a bulky side chain moiety on the backbone of the FPTA-3 polymer results in high charge density, more free volume, reduced chain packing of polymer segments inside the membrane matrix, and maximum gas transportation facilitation. The polymer's permeability and selectivity measurements are displayed in Table 6.

While the upstream feed pressure was gradually increased from 100 to 800 psi, the permeability coefficient of pure nitrogen gas increased slightly and the permeability coefficient of pure CH_4

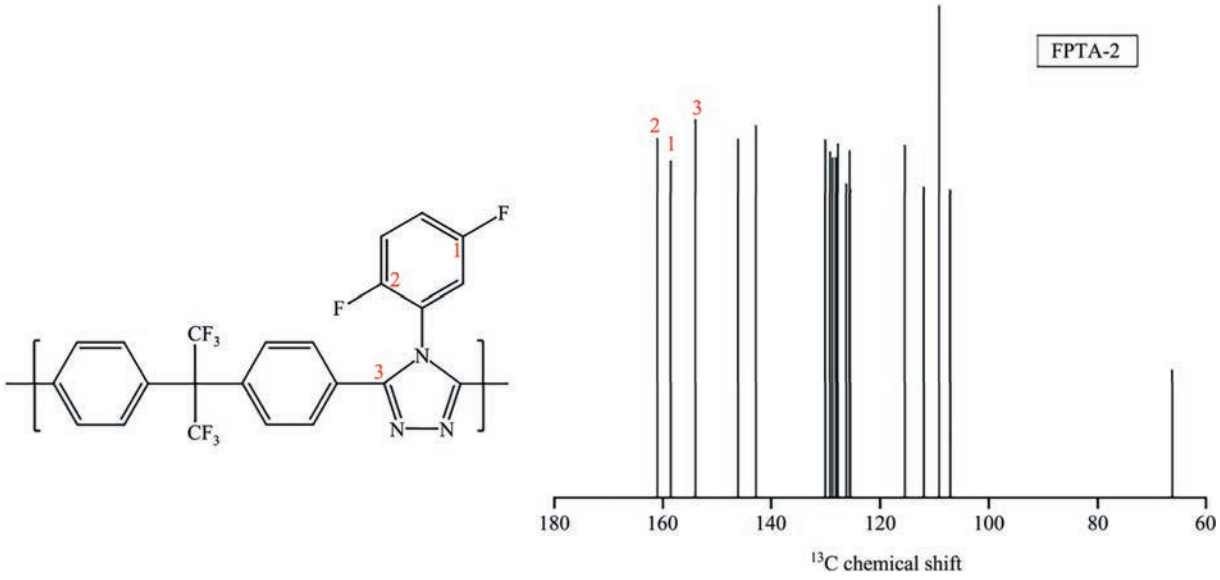

Fig. 11. Fluorinated polytriazole polymer's (FPTA-2) ^{13}C NMR spectra.

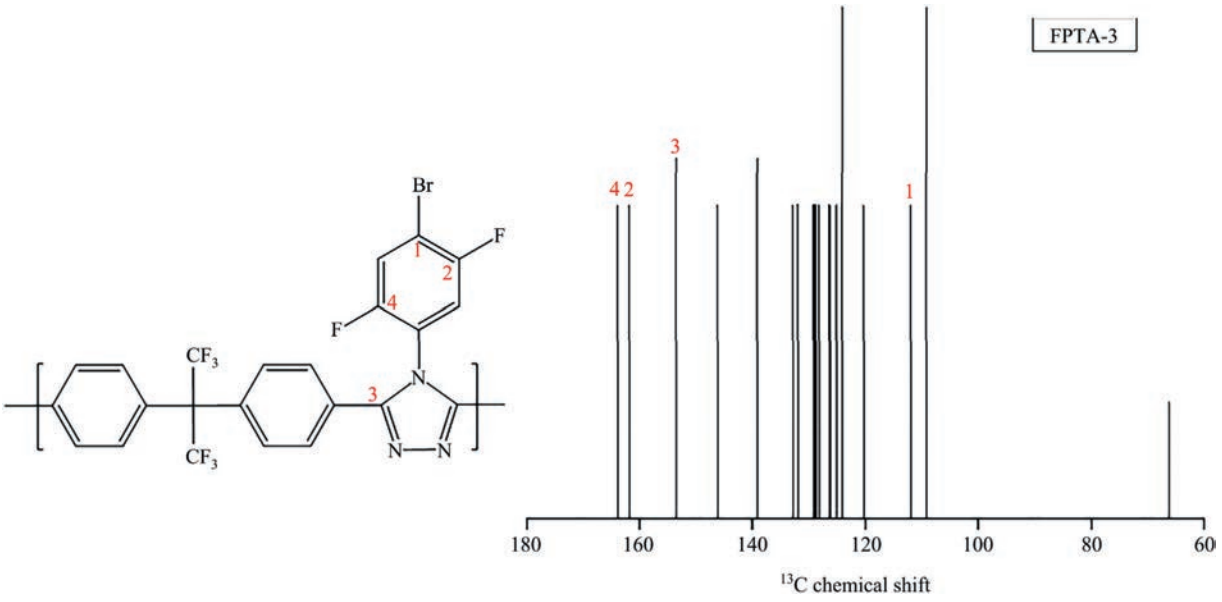

Fig. 12. Fluorinated polytriazole polymer's (FPTA-3) ^{13}C NMR spectra.

remained nearly constant for the membrane's materials made of polymer (FPTA-4). This behavior was observed in contrast to other membrane materials. With an increase in upstream input pressure from 100 to 800 psi, the permeabilities coefficient values obtained for the target single gases, such as CO_2 and He, were somewhat elevated. While the ideal selectivities of (He/CH_4) was constant throughout the applied pressure range (100 to 800 psi), the ideal selectivity of (CO_2/CH_4) was marginally reduced from 97 to 100. Under the applied upstream feed pressure range of 100 to 800 psi, there was an improvement in ideal selectivity and (CO_2/CH_4) due to the slight rise in the permeability of both CO_2 and He, and no change in the permeability values of both gases (N_2 and CH_4). We found that the polymer (FPTA-4) membrane materials performed much better than the polymers (FPTA-1, FPTA-2, and FPTA-3) membrane materials created and evaluated in this work in terms of permeability and selectivity towards natural gas purification by eliminating acid gas (CO_2) (Table 7).

The presence of five highly electronegative fluorine atoms (F) on the bulky side-chain aniline derivative in the backbone of the FPTA-4 polymer leads to an exceptionally high charge density within the polymer structure.

This strong electron-withdrawing effect significantly influences intermolecular interactions, dipole moments, and polymer chain rigidity, enhancing gas separation performance, thermal stability, and chemical resistance.

To systematically investigate the impact of fluorine content on polymer properties, different bulky fluorinated aniline derivatives were selected, with an increasing number of fluorine atoms progressing from FPTA-1 to FPTA-4. This gradual fluorine incorporation altered the polymer's free volume characteristics, molecular packing efficiency, and gas transport behavior. Due to the

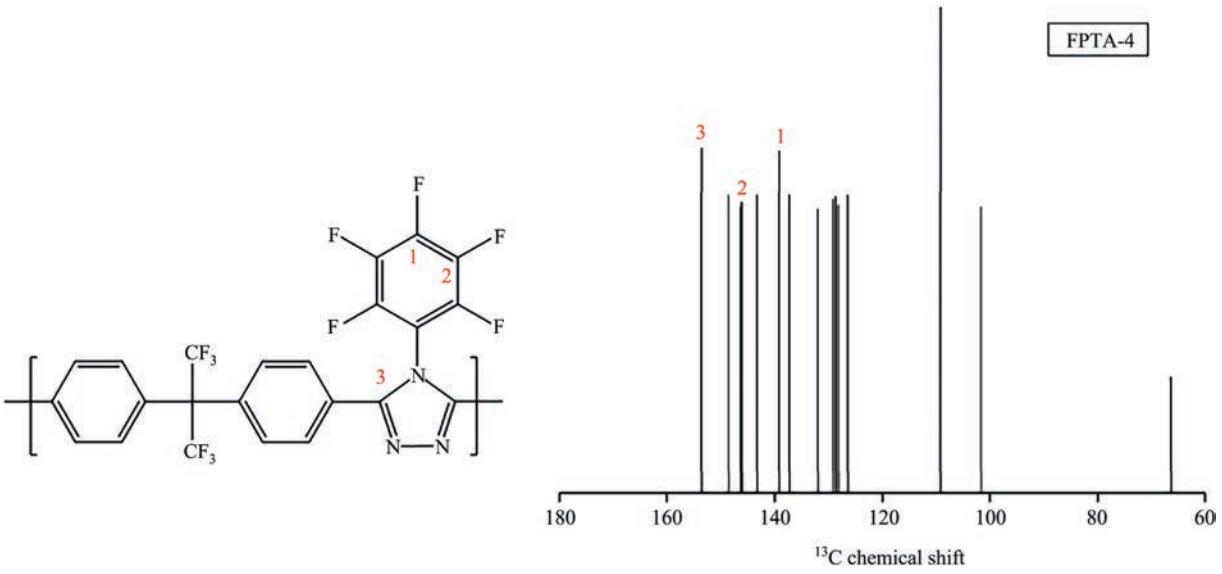

Fig. 13. Fluorinated polytriazole polymer's (FPTA-4) ^{13}C NMR spectra.

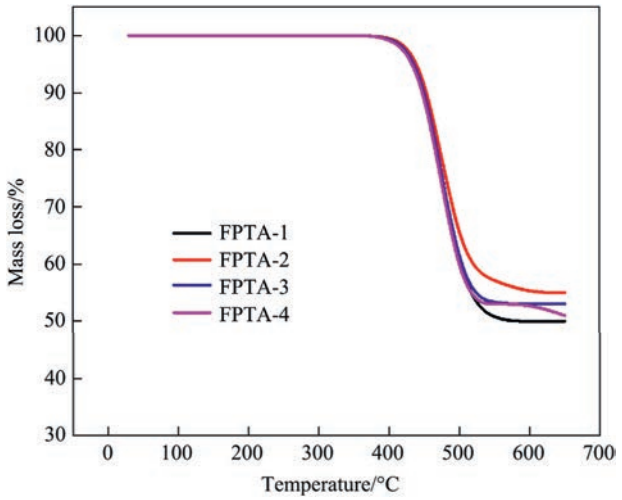

Fig. 14. Analyzing FPTA polymers thermogravimetrically (TGA).

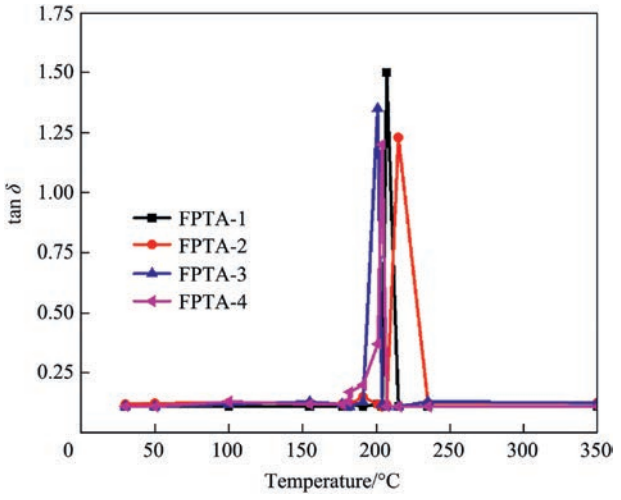

Fig. 15. Examination of FPTA polymers using dynamic mechanical thermal analysis (DMTA).

electrostatic charge repulsion between polymer segments, a significant free volume was created and increased, enhancing the overall gas permeability and diffusion properties. The increasing fluorine density contributed to improved CO_2 and He permeability, positioning FPTA-4 as a high-performance membrane material surpassing conventional commercial membranes.

The gas pair selectivity of CO_2/CH_4 is compared in Fig. 16 for both the single gas system and room temperature, with respect to the applied upstream feed pressure (100 to 800 psi). The fluorinated polymer membranes (FPTA-1, FPTA-2, and FPTA-3) produced for the CO_2/CH_4 gas pair exhibit a small drop in selectivity coefficient values when the applied feed pressure ranges from 100 to 800 psi. Simultaneously, the membranes derived from FPTA-4 polymer materials exhibit a slight increase in selectivity coefficient for the same gas pair (CO_2/CH_4) as the upstream feed pressure is gradually increased (from 100 to 800 psi) without exhibiting any indications of membrane swelling or plasticization. In contrast to other fluorinated polymer membrane materials, the selectivity of gas pair for this polymer membrane increased as a result of a slight increase in the permeability of CO_2 gas with an increase in pressure. Meanwhile, the permeability of CH_4 gas remained constant under the same upstream feed pressure from 100 to 800 psi.

The selectivity of the gas pair (He/CH_4) is compared in Fig. 17, where it is shown that when feed pressure increases from 100 to 800 psi, the selectivity coefficient values for the fluorinated polymer membrane materials derived from (FPTA-1 and FPTA-2) decrease noticeably. The permeability of CH_4 increased gradually from 2.7 to 4.30 Barrer and the permeability of He decreased somewhat under the same input pressure range (100 to 800 psi), which is the cause of this decline in selectivity coefficient values. In contrast to the other polymer membranes, the fluorinated polymer membranes made from FPTA-3 and FPTA-4 exhibit constant or very modest declines in the gas pair (He/CH_4) selectivity over the applied feed pressure range of 100 to 800 psi. The permeability of CH_4 increased gradually from 2.7 to 4.30 Barrer and the permeability of He gas decreased somewhat under the same input pressure range (100 to 800 psi), which is the cause of this decline in selectivity coefficient values. In contrast to the other polymer membranes, the fluorinated polymer membranes made from FPTA-3 and FPTA-4 exhibit constant or very modest declines in the selectivity of the gas pair (He/CH_4) over the applied feed pressure range of 100 to 800 psi. Under the same feed pressure range (100 to 800 psi), no apparent variation in the permeability values of either He or CH_4 was found.

3.2.2. The impact of temperature on a single gas' permeability

The solution-diffusion model is liable for the gas permeation process across dense polymeric membrane materials [29,36]. The upstream feed pressure, temperature, structural chemistry, and specific characteristics of the polymeric membrane materials all affect the permeability values for each gas. Arrhenius relationships can be used to explain how temperature affects a gas component's diffusivity (D), solubility (S), and permeability (P).

$$D = D_0 e^{-E_D / RT} \tag{5}$$

$$S = S_0 e^{-\Delta H_S / RT} \tag{6}$$

$$P = P_0 e^{-E_P / RT} \tag{7}$$

$$E_P = E_D + \Delta H_S \tag{8}$$

where P_0 (Barrer), S_0 ($cm^3(STP)\cdot cm^{-3}\cdot cmHg^{-1}$) and D_0 ($cm^2\cdot s^{-1}$) are pre-exponential factors. E_D ($kJ\cdot mol^{-1}$) is the activation energy of diffusion, R is the universal gas constant (8.314×10^{-3} $kJ\cdot mol^{-1}\cdot K^{-1}$), T (K) is the absolute temperature, ΔH_S ($kJ\cdot mol^{-1}$) represents the heat (enthalpy) of sorption and E_P ($kJ\cdot mol^{-1}$) is the activation energy for permeation.

Table 1
The FPTA polymer membrane materials' mechanical and thermal qualities.

FPTA polymers	T_g/°C	T_d at 5% mass loss (N_2)/°C	Char residue remaining at 650 °C/%	Densities of polymer membranes	FFV
FPTA-1	207.5	455	58	1.51	0.11
FPTA-2	200.5	485	56	1.47	0.15
FPTA-3	225.3	450	48	1.43	0.25
FPTA-4	204.3	485	51	1.35	0.31

Table 2
The FPTA polymers' molecular weight (M_W), degree of polymerization (DP), and polydispersity (PDI).

FPTA polymers	M_W/g·mol^{-1}	PDI	DP
FPTA-1	70000	2.1	151
FPTA-2	64000	2.3	133
FPTA-3	67000	2.2	119
FPTA-4	65000	2.2	122

Temperature change affects selectivity as well because a gas component's S and D are both temperatures dependent. Higher temperatures cause the segmental motion inside the membrane matrix to increase, which makes it more difficult for a membrane material to discriminate between gas components with differing physical dimensions. This reduces selectivity during gas diffusion. The solubility of gas components and the interactions between polymer and penetrant are also impacted by temperature variations. The selectivity of a gas depends on how much each gas component in the system is affected by temperature. For the majority of gases, solubilities decrease as temperature rises [19–29].

At various temperatures (25, 40, 50, and 60 °C) and upstream feed pressure of 200 psi, the impact of temperature on the membrane's performance in terms of permeability and selectivity of FPTA-1, FPTA-2, FPTA-3, and FPTA-4 was investigated. Table 8, Figs. 18 and 19, respectively, present the permeability coefficients of pure gases, such as He, CO_2, N_2, and CH_4, and the selectivity coefficients of gas pairs, such as (He/CH_4) and (CO_2/CH_4), as well as the Arrhenius parameters derived from Eq. (7). All of the single gases' permeability coefficients (He, CO_2, N_2, and CH_4) rose somewhat as temperature rose from 25 to 60 °C while maintaining the same upstream pressure of 200 psi. The kinetic diameter (size) of the gas component determines the E_P, which rises as the kinetic diameter of a penetrant gas increases. The single gases that were evaluated have the following orders of kinetic diameter: He (0.260 nm), CO_2 (0.330 nm), N_2 (0.364 nm), and CH_4 (0.380 nm). The permeability coefficient values for all the fluorinated polymer membranes developed in this research work, $P(He) > P(CO_2) > P(N_2) > P(CH_4)$, are in good agreement with the trend of activation energies for the permeation process, as shown in Table 8. $E_P(He) < E_P(CO_2) < E_P(N_2) < E_P(CH_4)$. Hence, compared to gas penetrants with larger kinetic diameters, those with smaller kinetic diameters activate more quickly. In addition, a rise in temperature has an impact on the mobility of the polymer chain, giving gas penetrant intersegmental jumps more room to occur. Consequently, the permeability and diffusion rates of gas penetrants increase with increasing temperature. But as the temperature range increased from 25 to 60 °C, the permeability coefficient values of single gases like He, CO_2, and CH_4 gradually increased, maintaining the selectivities for gas pairs like (He/CH_4) and (CO_2/CH_4). Because the permeability coefficients of CO_2 and He did not significantly rise with temperature, compared to CH_4, the selectivities values stayed constant. With temperature increases and the same upstream feed pressure of 200 psi, there was no discernible rise in the permeability coefficients of CO_2 and He relative to CH_4, which resulted in uniform selectivities values. Under the same feed pressure of 200 psi, the permeability and selectivity coefficients of the gases CO_2 and He increased steadily and steadily, demonstrating the special qualities of the fluorinated polymer materials that were synthesized and developed into membranes in this work. The temperature increased from 25 to 60 °C. The permeability and selectivity results were also compared to membrane materials described in the literature [29–33,35,37], where an increase in temperature causes a notable decrease in relevant selectivity but an increase in permeability. The reason for this property is explained by the resistance of the fluorinated polymer materials to permit restricted chain mobility within the polymer membrane matrix with temperature increases (25 to 60 °C) at feed pressures of 200 psi. The primary cause of the

Table 3
Single-gas permeability and selectivity coefficients at room temperature and 100 psi in FPTA polymer membranes.

Polyazole polymer membranes	Permeability/Barrer				Selectivity		
	N_2	CH_4	He	CO_2	N_2/CH_4	He/CH_4	CO_2/CH_4
FPTA-1	3.50	2.70	212.11	132.21	1.30	78.51	48.96
FPTA-2	3.11	2.35	285.55	185.23	1.30	105.55	78.82
FPTA-3	1.21	2.55	305.21	240.24	–	119.60	94.21
FPTA-4	4.13	3.10	395.31	303.25	–	127.41	97.82

Table 4
FPTA-1 at room temperature: single gas permeability and selectivity coefficients.

Upstream gas feed pressure/psi	Permeability/Barrer				Selectivity		
	N_2	CH_4	He	CO_2	N_2/CH_4	He/CH_4	CO_2/CH_4
100	3.50	2.70	212.10	132.10	1.30	78.51	48.88
300	4.25	2.71	211.20	131.11	1.56	77.85	48.38
600	4.55	4.30	211.05	131.07	1.05	49.06	30.48
800	4.72	4.30	210.10	125.11	1.09	48.83	29.09

Table 5
FPTA-2 at room temperature: single gas permeability and selectivity coefficients.

Upstream gas feed pressure/psi	Permeability/Barrer				Selectivity		
	N_2	CH_4	He	CO_2	N_2/CH_4	He/CH_4	CO_2/CH_4
100	3.11	2.35	285.55	185.23	1.35	121.50	78.82
300	3.11	2.33	280.31	176.45	1.33	120.30	75.72
600	3.10	2.33	277.30	155.51	1.33	119.01	66.74
800	3.10	2.33	275.65	145.35	1.32	118.30	62.38

Table 6
FPTA-3 at room temperature: single gas permeability and selectivity coefficients.

Upstream gas feed pressure/psi	Permeability/Barrer				Selectivity		
	N_2	CH_4	He	CO_2	N_2/CH_4	He/CH_4	CO_2/CH_4
100	1.21	2.55	305.21	240.24	–	119.69	94.21
300	1.11	2.55	303.25	235.23	–	118.92	92.24
600	1.10	2.60	295.15	233.30	–	113.51	89.73
800	1.00	2.65	295.11	231.13	–	111.36	87.21

Table 7
FPTA-4 at room temperature: single gas permeability and selectivity coefficients.

Upstream gas feed pressure/psi	Permeability/Barrer				Selectivity		
	N_2	CH_4	He	CO_2	N_2/CH_4	He/CH_4	CO_2/CH_4
100	4.13	3.10	395.31	303.25	1.33	127.31	97.82
300	4.25	3.12	396.25	307.23	1.36	127.00	98.47
600	4.31	3.12	396.15	310.33	1.38	126.15	99.47
800	4.33	3.13	397.11	313.13	1.38	126.87	100.04

modest rise in permeability coefficient values is the gas penetrants increased kinetic energy in the membrane matrix, which is unaffected by segmental chain mobility. For gas separation and purification under high pressure and temperature field processing for commercial applications, such polymer materials can be regarded as promising polymer membrane materials.

3.3. Fluorinated polymer membranes: mixed gas permeation experiments

For the synthesized fluorinated polymer membranes made from (FPTA-1, FPTA-2, FPTA-3, & FPTA-4) polymer materials, the permselectivity properties of a mixed gas system with composition (28.45% N_2; 60.38% CH_4; 0.97% C_2H_6; 10.19% CO_2) were assessed on a CP system at room temperature and under a range of upstream feed pressures of 100 to 800 psi.

Tables 9 and 10 below show the perm-selectivity performance of membranes made from FPTA-1 and FPTA-2 polymer materials, respectively. Under applied feed pressures ranging from 100 to 800 psi, the CO_2 permeability values for both membranes (FPTA-1 & FPTA-2) were found to be more selective toward CO_2 gas than other mixed gas components. These values were obtained for the single gases during a single gas permeation experiment. Under the same upstream input pressure (100 to 800 psi), the permeability coefficient values for CO_2 declined marginally, whereas the permeability coefficients for N_2, CH_4) and C_2H_6 increased significantly with pressure increases from 100 to 800. With an increase in the upstream feed pressure from 100 to 800 psi, the permeability of CO_2 gas decreased by 1.55% and 16.11%, respectively, for polymer membranes (FPTA-1 and FPTA-2). The primary cause is the low concentration (10% in mixture composition) of CO_2 gas, which results in low sorption. Additionally, the high kinetics of mixed gases under high upstream feed pressure range (100 to 800 psi) affect sorptive competition among the system's various gas constituents through the fluorinated polymer membrane. However, when the upstream input pressure was increased from 100 to 800 psi, the selectivity coefficients values of (CO_2/CH_4) fell for the FPTA-1 and FPTA-2 membrane materials, respectively, from 73.77 to 54.04 and 85.30 to 68.48. The reason for this decrease in selectivity is a small decrease in the permeability of CO_2, which is accompanied by an increase in the permeability coefficients of CH_4. However, compared to the single gas system, the selectivity coefficient values for the CO_2/CH_4 gas pair produced from the mixed gases system are significantly greater. Tables 9 and 10 below show the perm-selectivity results for the fluorinated polymer membranes (FPTA-1 & FPTA-2), respectively.

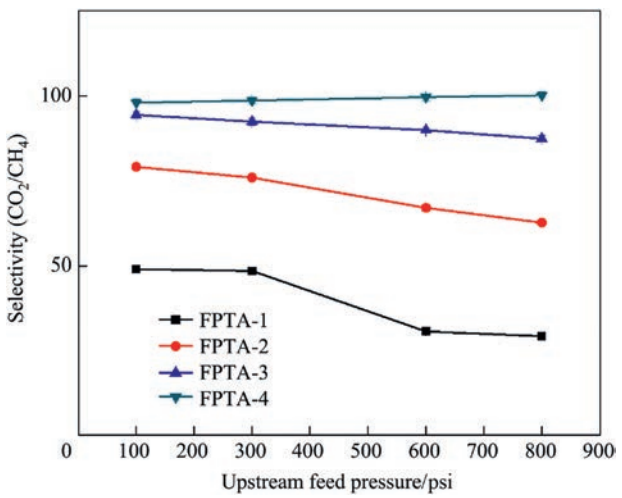

Fig. 16. Gas pair (CO_2/CH_4) selectivity as a function of feed pressure.

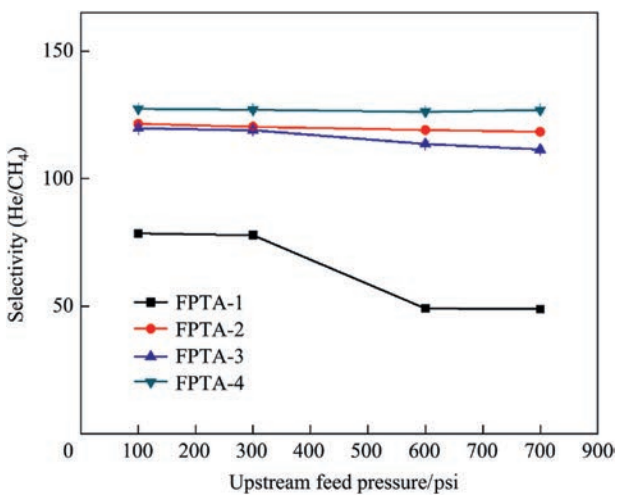

Fig. 17. Gas pair (He/CH_4) selectivity as a function of feed pressure.

Table 8
Permeation activation energies of the polymer membranes at 60 °C and 200 psi feed pressure.

Polymer membranes	Properties	He	CO_2	N_2	CH_4
FPTA-1	E_P/kJ·mol^{-1}	4.11	4.25	18.33	22.11
	P_0/Barrer	220.34	138.35	4.85	2.95
FPTA-2	E_P/kJ·mol^{-1}	3.55	3.85	21.75	22.50
	P_0/Barrer	282.35	180.31	3.55	2.51
FPTA-3	E_P/kJ·mol^{-1}	2.47	2.85	21.81	22.51
	P_0/Barrer	310.32	241.36	2.25	3.11
FPTA-4	E_P/kJ·mol^{-1}	2.45	2.51	21.88	22.71
	P_0/Barrer	401.22	322.35	4.11	4.10

Tables 11 and 12 below show the gas separation performance of membranes made from fluorinated polymer materials (FPTA-3 and FPTA-4). The CO_2 permeability values observed were found to be very close to the permeability coefficients obtained for the single gas permeation experiment over the upstream feed pressure range of 100 to 800 psi. This confirms the polymer material's selective nature toward CO_2 as compared to other gas components in the mixed gas system, such as CH_4, N_2, and C_2H_6. The permeability coefficient of pure nitrogen gas remained constant for the FPTA-3 polymer membrane, whereas the FPTA-4 membrane exhibited a slight decrease when the upstream feed pressure was increased from 100 to 800 psi. As the upstream input pressure was gradually increased from 100 to 800 psi, the permeability coefficient of pure CH_4 also marginally rose. Under the feed pressure range of 100 to 800 psi, the permeability coefficient of CH_4 was seen to rise up to 25% and 15%, respectively, for the FPTA-3 and FPTA-4 membranes. However, during the applied upstream feed pressure range of 100 to 800 psi, the permeability coefficient of CO_2 increased somewhat for both polymer membrane materials (FPTA-3 & FPTA-4), by 7% and 2.60%, respectively. With a rise in pressure from 99.57 to 80.19 for the FPTA-3 polymer membrane and from 109.09 to 94.76 for the FPTA-4 polymer membrane materials, the selectivity coefficient of the gas pair (CO_2/CH_4) dropped. The decrease in selectivities coefficient values can be attributed to a rise in CH_4 permeability, which is accompanied by a fall in CO_2 permeability within the same upstream input pressure range. The perm-selectivity results for the fluorinated polymer membranes (FPTA-3 & FPTA-4), respectively, are displayed in Tables 11 and 12.

Fig. 20 shows how the selectivity of a gas pair, such as CO_2/CH_4, *via* dense polymer membranes made from (FPTA-1 to FPTA-4), is affected by the upstream feed pressure from a mixed gas system. Upon fabrication and testing of all the fluorinated polymer membrane materials used in this study, the selectivity coefficient values fell. With a pressure increase from 100 to 800 psi and at room temperature, the decline in selectivities values was measured as 26.79% for (FPTA-1), 19.71% for (FPTA-2), 19.46% for (FPTA-3) and

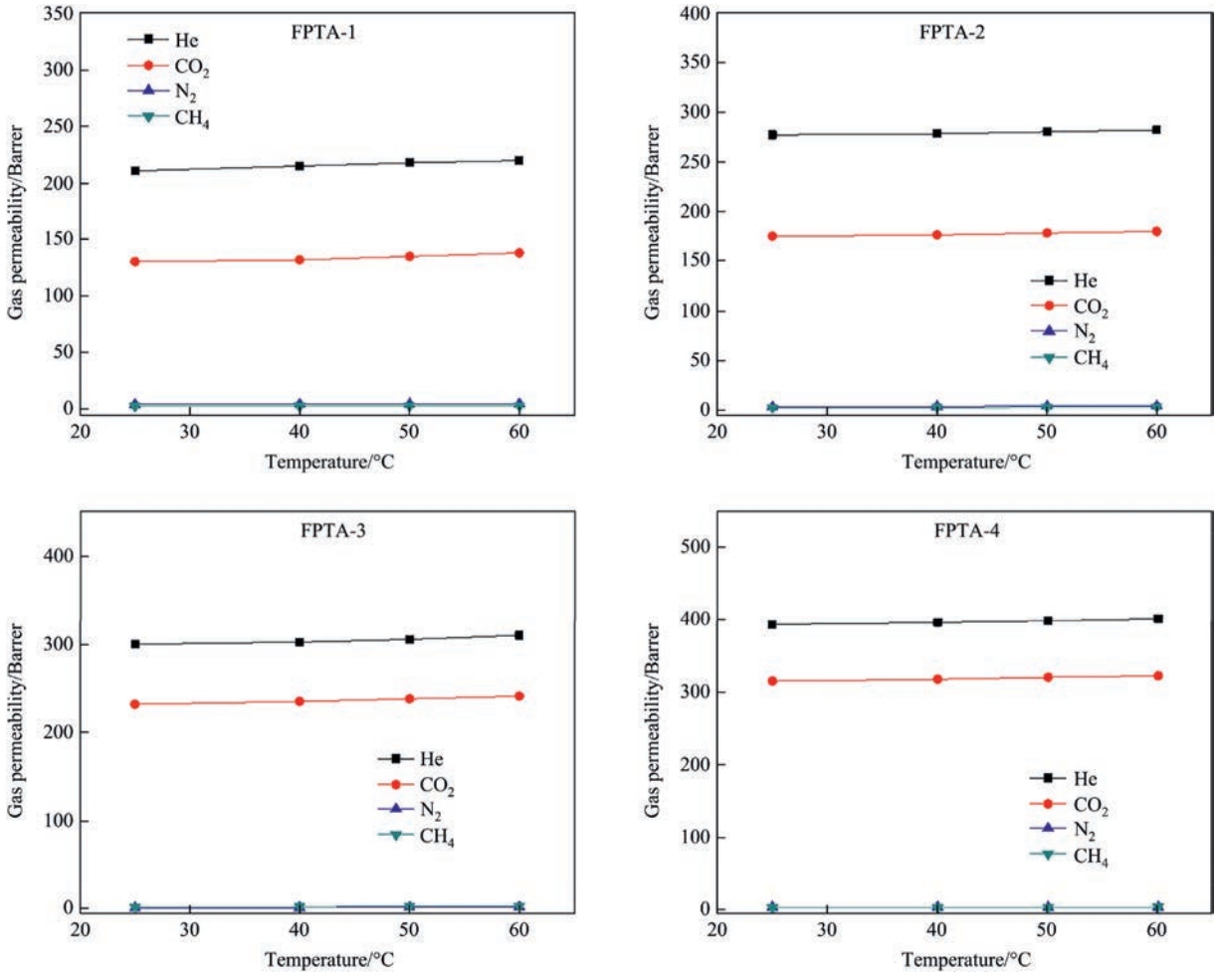

Fig. 18. Effects of activation energy on permeability of the membranes at 200 psi.

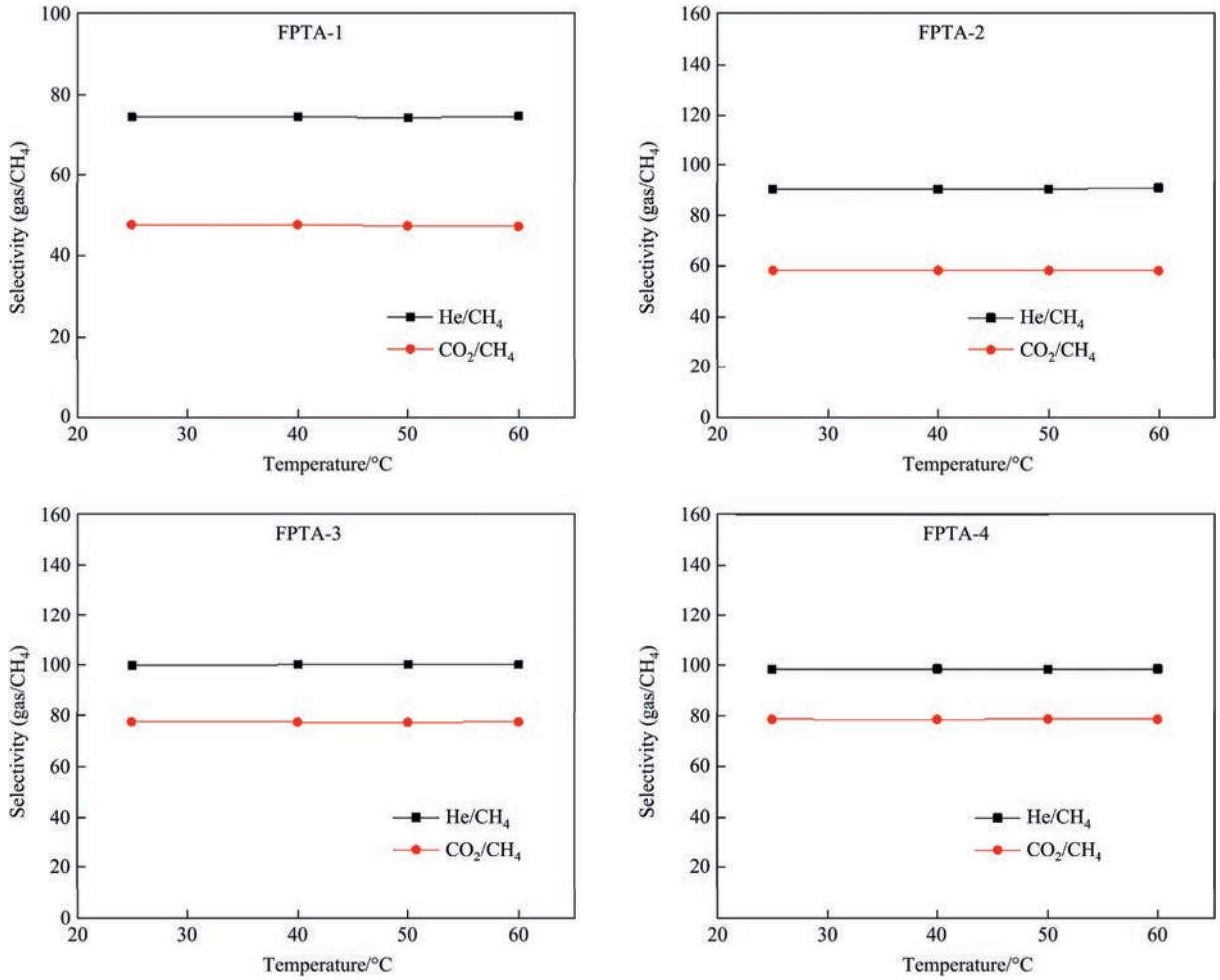

Fig. 19. Effects of activation energy on the selectivity of the membranes at 200 psi.

Table 9
FPTA-1: permeability and selectivity coefficients, gas mixture composition: 28.45% N_2; 60.38% CH_4; 0.97% C_2H_6; 10.19% CO_2.

Upstream gas feed pressure/psi	Permeability/Barrer				Selectivity	
	N_2	CH_4	C_2H_6	CO_2	N_2/CH_4	CO_2/CH_4
100	3.10	1.75	1.55	129.10	1.77	73.77
300	3.11	1.75	1.55	129.11	1.77	73.71
600	3.25	2.23	1.85	128.07	1.45	57.40
800	3.55	2.35	1.88	127.05	1.51	54.04

13.13% for (FPTA-4) membrane materials. The low concentration of CO_2 (10%) compared to the extremely high concentration of CH_4 (60%) and the sorptive competition among the gas components in the system which was previously discussed, are the primary causes of the decline in selectivities values. The synthesized and tested novel fluorinated polymer materials can be considered as commercially and economically feasible polymer membranes for natural gas field processing under high operating pressure (up to 800 psi), despite the fact that the perm-selectivity values obtained for the gas pair, such as CO_2/CH_4, are still very high.

3.4. Superior anti-plasticization characteristics of the new fluorinated polymer membrane materials

Induced gas penetrants, like CO_2, produce plasticization, or swelling, of the polymer membrane matrix due to polymer chain mobility. This invariably leads to low permselectivity for a target gas pair from the mixed gas system. These events happen when polymer membranes are put to the test in an experiment involving the purification and separation of gases (either mixed or single) under high upstream supply pressure [37–51]. The process of processing natural gas at high upstream feed pressure under CO_2 penetrant typically results in plasticization or swelling of polymer membranes. More studies on the plasticization of polymer membranes caused by CO_2 have been conducted, according to the literature. Being a highly condensable gas that causes swelling of the polymer membrane matrix at high upstream feed pressure and a sharp decline in permselectivity during mixed gas separation processes for industrial applications, CO_2 plasticization remains a significant difficulty even today. Many studies have been conducted over the years to suppress plasticization through the following methods: (1) blending different polymer materials; (2)

Table 10
FPTA-2: permeability and selectivity coefficients, gas mixture composition: 28.45% N_2; 60.38% CH_4; 0.97% C_2H_6; 10.19% CO_2.

Upstream gas feed pressure/psi	Permeability/Barrer				Selectivity	
	N_2	CH_4	C_2H_6	CO_2	N_2/CH_4	CO_2/CH_4
100	2.85	2.11	1.25	180.23	1.35	85.30
300	2.93	2.15	1.45	171.45	1.36	79.74
600	3.05	2.15	1.66	151.51	1.41	70.46
800	3.11	2.21	1.78	151.35	1.40	68.48

Table 11
FPTA-3: permeability and selectivity coefficients, gas mixture composition: 28.45% N_2; 60.38% CH_4; 0.97% C_2H_6; 10.19% CO_2.

Upstream gas feed pressure/psi	Permeability/Barrer				Selectivity	
	N_2	CH_4	C_2H_6	CO_2	N_2/CH_4	CO_2/CH_4
100	1.11	2.35	2.12	234.24	–	99.57
300	1.10	2.65	2.25	241.22	–	90.94
600	1.10	2.83	2.45	245.45	–	86.57
800	1.10	3.13	2.56	251.65	–	80.19

Table 12
FPTA-4: permeability and selectivity coefficients, gas mixture composition: 28.45% N_2; 60.38% CH_4; 0.97% C_2H_6; 10.19% CO_2.

Upstream gas feed pressure/psi	Permeability/Barrer				Selectivity	
	N_2	CH_4	C_2H_6	CO_2	N_2/CH_4	CO_2/CH_4
100	3.35	2.75	2.35	300.17	1.21	109.09
300	3.34	2.91	2.25	303.23	1.14	104.12
600	3.15	3.11	2.20	305.25	1.01	98.07
800	3.11	3.25	2.11	308.17	0.95	94.76

altering the membranes' surfaces; (3) crosslinking (ionic or covalent); (4) adding fillers to polymers and membranes (MOFs, CNT, ZIF, and so on); (5) thermally treating polymer membranes; and so forth [37–58]. Sadly, these kinds of alterations or treatments to polymers or membrane materials never succeeded in producing a polymer membrane material that shows promise in terms of permeability and selectivity during the high-pressure mixed gas separation process. Following these changes, the membranes were often either very low permeable with very high selectivity or more permeable with very low selectivity. Membrane materials for commercial applications need to possess special qualities including high permeability and strong selectivity for the target gas pair in the mixed gas system and composition.

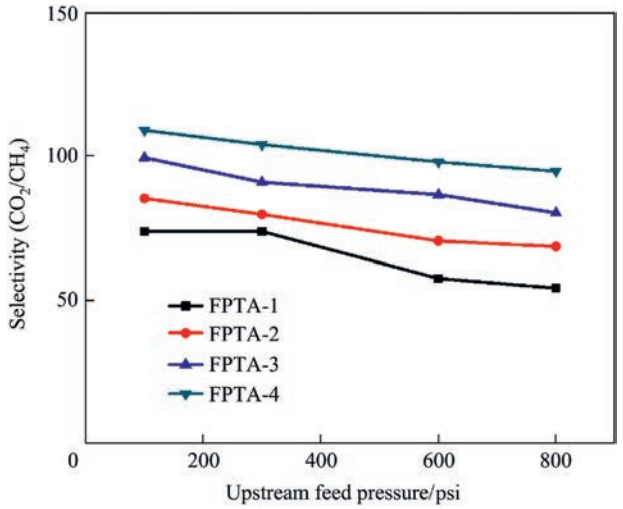

Fig. 20. Gas pair (CO_2/CH_4) selectivities as a function feed pressure from a mixed gas system (28.45% N_2; 60.38% CH_4; 0.97% C_2H_6; 10.19% CO_2).

Utilizing a single, pure CO_2 permeance at a high upstream feed pressure range (100 to 800 psi), the anti-plasticization performance of the membranes developed in this research work from the synthesized fluorinated polymers (FPTA-1 to FPTA-4) was experimentally examined. The polymer membranes were tested for a total of 24 h under each pressure. The anti-plasticization behavior of the synthesized fluorinated polymer membrane materials (FPTA-1 to FPTA-4) at room temperature (a) and at varying temperatures (25°C to 60 °C) (b) under the high feed pressure range (100 to 800 psi) of a single gas (CO_2). Under applied upstream feed pressure range of 100 to 800 psi, the permeability coefficients of pure CO_2 gas obtained from the single gas permeation experiments (Fig. 21(a)) remain constant for (FPTA-1 & FPTA-3) polymer membrane materials, slightly increased for (FPTA-4) membrane materials, and decreased for (FPTA-2) polymer membranes. This demonstrates the newly created fluorinated polymer membrane materials with excellent mechanical and chemical durability that do not expand or dilate in the severe, acidic CO_2 environment. All of the synthetic polymer membranes, on the other hand, showed distinct behavior (Fig. 21(b)), with the permeabilities values marginally increasing with temperature at the same upstream feed pressure of 200 psi. The cause of this increase in selectivity values was a minor increase in both gases' (CO_2 & CH_4) permeability coefficients at the same time as a rise in their kinetic energy brought about by the gases' progressive rise in temperature from 25 to 60 °C at the same pressure of 200 psi.

In all cases, the single and mixed gas permeation trials revealed no defects resulting from the dilatation or swelling of the polymer membrane matrix. The HFA moiety on the polymer backbone and the bulky fluorinated triazole ring as side chain are responsible for these characteristics. These novel fluorinated polymer materials, which were synthesized and developed into dense membranes in

this research effort, can be regarded as potential membrane materials for high pressure natural gas processing on field application due to their distinctive features. This high upstream feed pressure of CO_2 gas (single or mixed gas system) and the anti-plasticization property of the polymer membrane materials are exclusive when compared to those documented in the literature [39–45], whereby the treated commercial polymer membrane began to plasticize as soon as the CO_2 gas feed pressure increased to 300 psi.

3.5. Comparison with trade-off curve

Plotting the novel synthesized fluorinated polymers membrane materials in this research work's gas purification and separation performance against commercially available polymers membrane materials like PDMS, Matrimid, polyimides, cellulose acetate, Pebax, and mixed matrix membranes (MMM) [32–38] on the upper bound trade-off lines [35,43] is illustrated in Fig. 22. The Robeson upper bound curves (1991 & 2008) were used for comparison. The polymer membranes' performance in separating CO_2 as a single gas is compared across the curves. When it comes to performance, all of the fluorinated polymer membranes (FPTA-1 through FPTA-4) surpass the 2008 trade-off line and are therefore

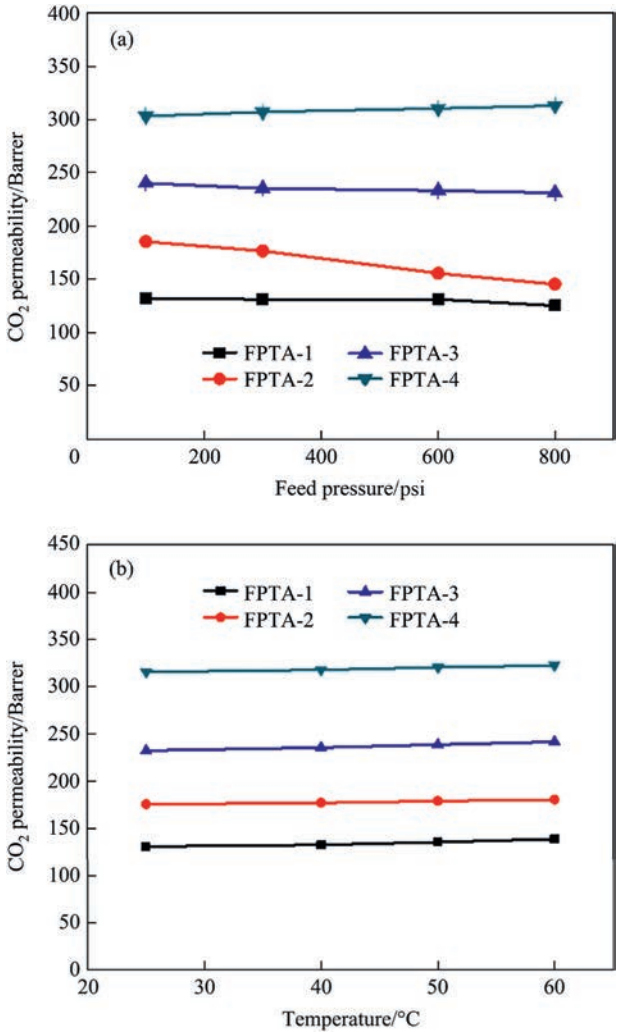

Fig. 21. High fluorinated polymer anti-plasticization properties: (a) with pure CO_2 gas fed at high pressures between 100 and 800 psi, and (b) at different temperatures between 25°C and 60 °C at 200 psi.

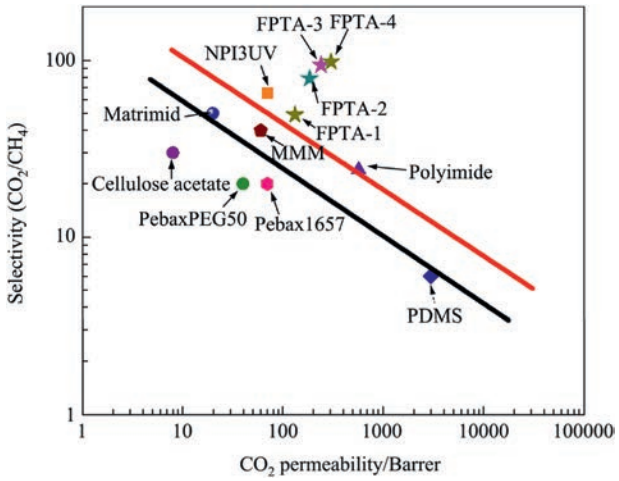

Fig. 22. Comparing membranes using trade-off curves (CO_2 gas); Robeson upper bound (black line) 1991; Robeson upper bound (red line) 2008.

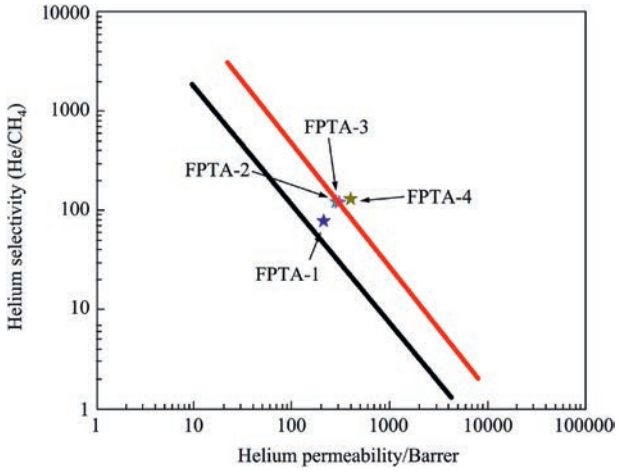

Fig. 23. Comparing membranes using trade-off curves (He gas); Robeson upper bound (black line) 1991; Robeson upper bound (red line) 2008.

in the running to be the best polymer membranes that have been documented in the literature [48–63]. Research is still being done to further improve the membranes' performance through the creation of composite membranes on the currently woven support. This will enable the membranes to be produced in large quantities for use in high-pressure natural gas processing for commercial purposes on gas fields. Additionally, creating polytriazole polymers with bulkier (fluorinated and non-fluorinated) groups as a side chain can boost the gas solubility and diffusion of CO_2 with high permeability and selectivity, as well as yield more free volume.

The Robeson plots for He/CH_4 are compared with the perm-selectivity performance of the recently developed fluorinated polymer membranes in Fig. 23. Only one polymer membrane (FPTA-1) crosses the Robeson trade-off curve in terms of performance in 1991, according to the plotted data. Two polymer membranes (FPTA-2 & FPTA-3) enter the Robeson trade-off line in 2008, and one polymer membrane (FPTA-4) has already crossed the trade-off line in 2008. In order to extract and purify He from natural gas, no glassy membrane materials have, as far as we are aware, been commercialized. Therefore, it is anticipated that the glassy polymeric materials for He separation and purification

developed in this study will be a focus of ongoing research for the procedures involved in recovering and separating He gas. More attention will be paid to the synthesis of polymers with novel chemistries and morphologies in order to develop an effective membrane material that is highly selective for the gas pair (He/CH_4) and has good permeability.

4. Conclusions

Through the method of polycondensation polymerization, FPTA polymers with specific chemistries were synthesized from chosen monomers. The production of membranes was made simple by the casting technique of polymer solution followed by solvent evaporation at room temperature or, in the case of high boiling solvents, at a high temperature. All of the synthesized FPTA polymers were highly soluble in the majority of common organic solvents at room temperature. In contrast to other gases like CH_4, C_2H_6, and N_2, the FPTA polymers with HFA in the main stem and bulky fluorinated aniline derivative as a side chain produced significantly higher permeability and selectivity of He and CO_2, according to single and mixed gas results. Very similar perm-selectivity values were found for CO_2 in the mixed gas system as compared to the single and pure gas system studies. As no swelling or dilatation of the membranes was noticed during testing of pure and mixed (CO_2) gas experiments at varying temperatures (25 to 60 °C) and high pressures (100 to 800 psi), the newly developed fluorinated polymer membranes demonstrated high mechanical stability and anti-plasticization properties.

Future research will focus on the development of a composite membrane incorporating an ultrathin (~1 μm) selective layer of FPTA polymer deposited on a robust non-woven support. This design aims to enable scalability for commercial applications and compatibility with mass production processes. The membrane will be engineered for the efficient separation and purification of CO_2 and He gases. Special emphasis will be placed on achieving high selectivity for CO_2/CH_4 and He/CH_4 gas pairs, targeting applications in natural gas upgrading, carbon capture, and He recovery.

CRediT Authorship Contribution Statement

Husnul Maab: Writing – review & editing, Writing – original draft, Validation, Supervision, Resources, Project administration, Methodology, Investigation, Conceptualization. Azra Touheed: Writing – original draft, Software, Methodology, Formal analysis, Data curation. Salman Salman: Writing – original draft, Methodology, Formal analysis, Data curation, Conceptualization. Maaz Khan: Writing – original draft, Software, Formal analysis, Data curation.

Declaration of Competing Interest

The authors declare the following financial interests/personal relationships which may be considered as potential competing interests:I am the Corresponding author for this manuscript and declare no conflict of interest related to this article submitted to Chemical Engineering JournalHusnul Maab If there are other authors, they declare that they have no known competing financial interests or personal relationships that could have appeared to influence the work reported in this paper.

References

[1] T.S. Chung, Commercial polymeric membrane for gas separation, *Encyclopedia* 1 (1) (2021) 18076.
[2] R.W. Baker, K. Lokhandwala, Natural gas processing with membranes: an overview, *Ind. Eng. Chem. Res.* 47 (7) (2008) 2109–2121.
[3] B. Kraftschik, W.J. Koros, J.R. Johnson, O. Karvan, Dense film polyimide membranes for aggressive sour gas feed separations, *J. Membr. Sci.* 428 (2013) 608–619.
[4] Z.E. Zhang, A. Fuoco, G.W. He, Membranes for gas separation, *Membranes* 11 (10) (2021) 755.
[5] F.M. Benedetti, M.G. De Angelis, M.D. Esposti, P. Fabbri, A. Masili, A. Orsini, A. Pettinau, Enhancing the separation performance of glassy PPO with the addition of a molecular sieve (ZIF-8): gas transport at various temperatures, *Membranes* 10 (4) (2020) 56.
[6] R.J. Hou, S.J.D. Smith, K. Konstas, C.M. Doherty, C.D. Easton, J. Park, H. Yoon, H. T. Wang, B.D. Freeman, M.R. Hill, Synergistically improved PIM-1 membrane gas separation performance by PAF-1 incorporation and UV irradiation, *J. Mater. Chem. A* 10 (18) (2022) 10107–10119.
[7] S. Zhao, J. Liao, D. Li, X. Wang, N. Li, Blending of compatible polymer of intrinsic microporosity (PIM-1) with Tröger's base polymer for gas separation membranes, *J. Membr. Sci.* 566 (2018) 77–86.
[8] R. Swaidan, M. Al-Saeedi, B. Ghanem, E. Litwiller, I. Pinnau, Rational design of intrinsically ultra microporous polyimides containing bridgehead-substituted triptycene for highly selective and permeable gas separation membranes, *Macromolecules* 47 (15) (2014) 5104–5114.
[9] W.J. Koros, G.K. Fleming, Membrane-based gas separation, *J. Membr. Sci.* 83 (1) (1993) 1–80.
[10] C.J. Orme, F.F. Stewart, Mixed gas hydrogen sulfide permeability and separation using supported polyphosphazene membranes, *J. Membr. Sci.* 253 (1–2) (2005) 243–249.
[11] G. Chatterjee, A.A. Houde, S.A. Stern, Poly(ether urethane) and poly(ether urethane urea) membranes with high H_2S/CH_4 selectivity, *J. Membr. Sci.* 135 (1) (1997) 99–106.
[12] X. Chen, G.P. Liu, W.Q. Jin, Natural gas purification by asymmetric membranes: an overview, *Green Energy Environ.* 6 (2) (2021) 176–192.
[13] T. Mohammadi, M.T. Moghadam, M. Saeidi, M. Mahdyarfar, Acid gas permeation behavior through poly(ester urethane urea) membrane, *Ind. Eng. Chem. Res.* 47 (19) (2008) 7361–7367.
[14] W.L. Qiu, C.C. Chen, L.R. Xu, L.L. Cui, D.R. Paul, W.J. Koros, Sub-Tg cross-linking of a polyimide membrane for enhanced CO_2 plasticization resistance for natural gas separation, *Macromolecules* 44 (15) (2011) 6046–6056.
[15] L. Yin, D.F. Li, H.X. Guo, S. Wang, T.X. Zhang, Y.L. Liu, F.Y. Gai, X.G. Zhao, High-performance carbonized ZIF-8-doped hybrid carbon molecular sieve membrane for CO_2/N_2 separation, *J. Membr. Sci.* 655 (2022) 120610.
[16] E. Lasseuguette, B. Comesaña-Gándara, Polymer membranes for gas separation, *Membranes* 12 (2) (2022) 207.
[17] A. Bos, I.G.M. Pünt, M. Wessling, H. Strathmann, CO_2-induced plasticization phenomena in glassy polymers, *J. Membr. Sci.* 155 (1) (1999) 67–78.
[18] G. Genduso, I. Pinnau, Quantification of sorption, diffusion, and plasticization properties of cellulose triacetate films under mixed-gas CO_2/CH_4 environment, *J. Membr. Sci.* 610 (2020) 118269.
[19] Y.Y. Zhang, X. Feng, S. Yuan, J.W. Zhou, B. Wang, Challenges and recent advances in MOF–polymer composite membranes for gas separation, *Inorg. Chem. Front.* 3 (7) (2016) 896–909.
[20] G. Genduso, Y.G. Wang, B.S. Ghanem, I. Pinnau, Permeation, sorption, and diffusion of CO_2–CH_4 mixtures in polymers of intrinsic microporosity: the effect of intrachain rigidity on plasticization resistance, *J. Membr. Sci.* 584 (2019) 100–109.
[21] E.R. Hensema, B. Gebben, M.H.V. Mulder, C.A. Smolders, Polyoxadiazoles and polytriazoles as new heat and solvent resistant membrane materials, *Bull. Des Sociétés Chim. Belg.* 100 (2) (1991) 129–136.
[22] H. Maab, L. Francis, A. Al-saadi, C. Aubry, N. Ghaffour, G. Amy, S.P. Nunes, Synthesis and fabrication of nanostructured hydrophobic polyazole membranes for low-energy water recovery, *J. Membr. Sci.* 423 (2012) 11–19.
[23] H. Maab, A. Al Saadi, L. Francis, S. Livazovic, N. Ghafour, G.L. Amy, S.P. Nunes, Polyazole hollow fiber membranes for direct contact membrane distillation, *Ind. Eng. Chem. Res.* 52 (31) (2013) 10425–10429.
[24] G. Matar, G. Gonzalez-Gil, H. Maab, S. Nunes, P. Le-Clech, J. Vrouwenvelder, P. E. Saikaly, Temporal changes in extracellular polymeric substances on hydrophobic and hydrophilic membrane surfaces in a submerged membrane bioreactor, *Water Res.* 95 (2016) 27–38.
[25] H. Maab, S.P. Nunes, Porous polyoxadiazole membranes for harsh environment, *J. Membr. Sci.* 445 (2013) 127–134.
[26] S.P. Nunes, H. Maab, L. Francis, Membrane for water purification, US Pat. 0179450 A1 (2021).
[27] S.P. Nunes, H. Maab, L. Francis, Polyazole membrane for water purification, Eur. Pat. 2626127 B1 (2013).
[28] E.R. Hensema, M.E.R. Sena, M.H.V. Mulder, C.A. Smolders, Gas separation properties of new polyoxadiazole and polytriazole membranes, *Gas Sep. Purif.* 8 (3) (1994) 149–160.
[29] E.R. Hensema, Polymeric gas separation membranes, *Adv. Mater.* 6 (4) (1994) 269–279.
[30] B. Gebben, M.H.V. Mulder, C.A. Smolders, Gas separation properties of a thermally stable and chemically resistant polytriazole membrane, *J. Membr. Sci.* 46 (1) (1989) 29–41.
[31] S. Chisca, N.M.S. Bettahalli, V.E. Musteata, S. Vasylevskyi, M.N. Hedhili, E. Abou-Hamad, M. Karunakaran, G. Genduso, S.P. Nunes, Thermal treatment

of hydroxyl functionalized polytriazole and its effect on gas transport: from crosslinking to carbon molecular sieve, *J. Membr. Sci.* 642 (2022) 119963.
[32] H. Maab, E. Qasem, Fluorinated polytriazole membrane materials for gas separation technology, US Pat., 10,919,002 B2 (2018).
[33] H. Maab, A. Touheed, Polyazole polymers membranes for high pressure gas separation technology, *J. Membr. Sci.* 642 (2022)119980.
[34] H. Maab, Polytriazole coating materials for metal substrate, US Pat. 0017774 A1 (2022).
[35] H. Maab, Polytriazole copolymers composition, US Pat. 0017688 A1 (2022).
[36] A. Bondi, Van der Waals volumes and radii, *J. Phys. Chem.* 68 (3) (1964) 441–451.
[37] D.W. Van Krevelen, K. Te Nijenhuis, Properties of Polymers: Their Correlation with Chemical Structure; Their Numerical Estimation and Prediction from Additive Group Contributions, fourth ed., Elsevier, Amsterdam, 2009.
[38] Y.H. Zhao, M.H. Abraham, A.M. Zissimos, Fast calculation of van der Waals volume as a sum of atomic and bond contributions and its application to drug compounds, *J. Org. Chem.* 68 (19) (2003) 7368–7373.
[39] G.O. Yahaya, I. Mokhtari, A.A. Alghannam, S.H. Choi, H. Maab, A.A. Bahamdan, Cardo-type random co-polyimide membranes for high pressure pure and mixed sour gas feed separations, *J. Membr. Sci.* 550 (2018) 526–535.
[40] J.G. Wijmans, R.W. Baker, The solution-diffusion model: a review, *J. Membr. Sci.* 107 (1–2) (1995) 1–21.
[41] M.L. Zhang, L.M. Deng, D.X. Xiang, B. Cao, S.S. Hosseini, P. Li, Approaches to suppress CO_2-induced plasticization of polyimide membranes in gas separation applications, *Processes* 7 (1) (2019) 51.
[42] M.M. Rahman, C. Abetz, S. Shishatskiy, J. Martin, A.J. Müller, V. Abetz, CO_2 selective polyactive membrane: thermal transitions and gas permeance as a function of thickness, *ACS Appl. Mater. Interfaces* 10 (31) (2018) 26733–26744.
[43] S. Chisca, P.H.H. Duong, A.H. Emwas, R. Sougrat, S.P. Nunes, Crosslinked copolyazoles with a zwitterionic structure for organic solvent resistant membranes, *Polym. Chem.* 6 (4) (2015) 543–554.
[44] S. Chisca, G. Falca, V.E. Musteata, C. Boi, S.P. Nunes, Crosslinked polytriazole membranes for organophilic filtration, *J. Membr. Sci.* 528 (2017) 264–272.
[45] W.J. Koros, G.K. Fleming, S.M. Jordan, T.H. Kim, H.H. Hoehn, Polymeric membrane materials for solution-diffusion based permeation separations, *Prog. Polym. Sci.* 13 (4) (1988) 339–401.
[46] M.R. Pixton, D.R. Paul, Relationships between structure and transport properties for polymers with aromatic backbones, in: D.R. Paul, Y. Yampolskii (Eds.), Polymeric Gas Separation Membranes, CRC Press, Boca Raton, 1994.
[47] J.H. Petropoulos, Mechanisms and theories for sorption and diffusion of gases in polymers, in: D.R. Paul, Y. Yampolskii (Eds.), Polymeric Gas Separation Membranes, CRC Press, Boca Raton, 1994.
[48] M. Wessling, S. Schoeman, T. van der Boomgaard, C.A. Smolders, Plasticization of gas separation membranes, *Gas Sep. Purif.* 5 (4) (1991) 222–228.2
[49] J.K. Adewole, A.L. Ahmad, S. Ismail, C.P. Leo, Current challenges in membrane separation of CO_2 from natural gas: a review, *Int. J. Greenh. Gas Control* 17 (2013) 46–65.
[50] A. Car, C. Stropnik, W. Yave, K.V. Peinemann, Pebax®/polyethylene glycol blend thin film composite membranes for CO_2 separation: performance with mixed gases, *Sep. Purif. Technol.* 62 (1) (2008) 110–117.
[51] L.M. Robeson, The upper bound revisited, *J. Membr. Sci.* 320 (1–2) (2008) 390–400.
[52] H. Maab, M. Schieda, W. Yave, S. Shishatskiy, S.P. Nunes, SPEEK/polyimide blends for proton conductive membranes, *Fuel Cells* 9 (4) (2009) 401–409.
[53] C.Q. Liu, S.T. Wilson, J.J. Chiou, D.A. Lesch, S. Kulprathipanja, Plasticization resistant membranes, US Pat., 0326273 A1 (2010).
[54] C.Q. Liu, S.T. Wilson, D.A. Lesch, High plasticization-resistant cross-linked polymeric membranes for separation, US Pat. 0318620 A1 (2009).
[55] W.J. Koros, De Q. Vu, R. Mahajan, S.J. Miller, Gas separations using mixed matrix membranes, US Pat., 6503295 B1 (2003).
[56] Y. Han, W.S. Winston Ho, Recent advances in polymeric membranes for CO_2 capture, *Chin. J. Chem. Eng.* 26 (11) (2018) 2238–2254.
[57] K.V. Peinemann, G. Johannsen, W.Y. Rios, A. Cai, Polymer membrane, US Pat., 8317900 B2 (2012).
[58] B. Bikson, Y. Ding, J.K. Leroux, J.K. Nelson, Gas separation using membranes formed from blends of perfluorinated polymers, US Pat., 6723152 B2 (2004).
[59] C.Q. Liu, T.C. Bowen, E.G. Harbert, R. Minkov, S.A. Faheem, Z. Osman, Process of separating gases using polyimide membranes, US Pat., 8704030 B2 (2014).
[60] B. Comesaña-Gándara, J. Chen, C.G. Bezzu, M. Carta, I. Rose, M.C. Ferrari, E. Esposito, A. Fuoco, J.C. Jansen, N.B. McKeown, Redefining the Robeson upper bounds for CO_2/CH_4 and CO_2/N_2 separations using a series of ultra permeable benzotriptycene-based polymers of intrinsic microporosity, *Energy Environ. Sci.* 12 (9) (2019) 2733–2740.
[61] S. Xu, X.L. Ren, N. Zhao, L. Wu, Z.G. Zhang, Y.F. Fan, N.W. Li, Self-crosslinking of bromomethylated 6FDA-DAM polyimide for gas separations, *J. Membr. Sci.* 636 (2021) 119534.
[62] R. Sidhikku Kandath Valappil, N. Ghasem, M. Al-Marzouqi, Current and future trends in polymer membrane-based gas separation technology: a comprehensive review, *J. Ind. Eng. Chem.* 98 (2021) 103–129.
[63] Y. Rogan, R. Malpass-Evans, M. Carta, M. Lee, J.C. Jansen, P. Bernardo, G. Clarizia, E. Tocci, K. Friess, M. Lanč, N.B. McKeown, A highly permeable polyimide with enhanced selectivity for membrane gas separations, *J. Mater. Chem. A* 2 (14) (2014) 4874–4877.